Article

Amygdala inhibitory neurons as loci for translation in emotional memories

https://doi.org/10.1038/s41586-020-2793-8

Received: 28 June 2019

Accepted: 6 July 2020

Published online: 7 October 2020

Check for updates

Prerana Shrestha[1]✉, Zhe Shan[1], Maggie Mamcarz[1], Karen San Agustin Ruiz[1], Adam T. Zerihoun[1], Chien-Yu Juan[1], Pedro M. Herrero-Vidal[1], Jerry Pelletier[2], Nathaniel Heintz[3] & Eric Klann[1,4]✉

To survive in a dynamic environment, animals need to identify and appropriately respond to stimuli that signal danger[1]. Survival also depends on suppressing the threat-response during a stimulus that predicts the absence of threat (safety)[2–5]. An understanding of the biological substrates of emotional memories during a task in which animals learn to flexibly execute defensive responses to a threat-predictive cue and a safety cue is critical for developing treatments for memory disorders such as post-traumatic stress disorder[5]. The centrolateral amygdala is an important node in the neuronal circuit that mediates defensive responses[6–9], and a key brain area for processing and storing threat memories. Here we applied intersectional chemogenetic strategies to inhibitory neurons in the centrolateral amygdala of mice to block cell-type-specific translation programs that are sensitive to depletion of eukaryotic initiation factor 4E (eIF4E) and phosphorylation of eukaryotic initiation factor 2α (p-eIF2α). We show that de novo translation in somatostatin-expressing inhibitory neurons in the centrolateral amygdala is necessary for the long-term storage of conditioned-threat responses, whereas de novo translation in protein kinase Cδ-expressing inhibitory neurons in the centrolateral amygdala is necessary for the inhibition of a conditioned response to a safety cue. Our results provide insight into the role of de novo protein synthesis in distinct inhibitory neuron populations in the centrolateral amygdala during the consolidation of long-term memories.

Neurons have evolved both to respond dynamically to their environment at millisecond time scales and to store information stably for a much longer period of time. The stabilization of information during mnemonic processes requires de novo translation[10,11]. Translation is tightly regulated during its initiation, when the two main rate-limiting steps are the assembly of the eIF2–$tRNA_i^{Met}$ ternary complex and the ^{m7}GpppN cap-binding complex[12]. Bidirectional control of protein synthesis can be mediated by altering the levels of these two complexes. As part of the integrated stress response, eIF2α kinases phosphorylate eIF2α and this in turn inhibits the eIF2 guanine exchange factor eIF2B, effectively blocking recycling of the ternary complex to prevent general translation. On the other hand, eIF2α is dephosphorylated after memory formation, allowing initiation of the requisite de novo translation[13]. Likewise, the formation of the ^{m7}GpppN cap-binding complex is essential for the initiation of cap-dependent translation. The regulation of cap-dependent translation relies on the mammalian target of rapamycin complex I (mTORC1) signalling pathway. Activation of mTORC1 triggers the initiation of cap-dependent translation through the phosphorylation of eIF4E-binding proteins (4E-BPs) and p70 S6 kinase 1 (S6K1). The phosphorylation of 4E-BPs results in the release of eIF4E, which then becomes incorporated into the eIF4F complex, along with the modular scaffolding protein eIF4G and the RNA helicase eIF4A to initiate cap-dependent translation. Phosphorylation of S6K1 leads to phosphorylation of downstream targets, including ribosomal protein S6, eIF4B, and PDCD4, that promote translation[12,14]. Although both the eIF2 and mTORC1 pathways regulate key steps in the initiation of translation, they are generally viewed as separate translation control pathways with largely non-overlapping molecular outcomes[15,16].

We developed a differential threat-conditioning paradigm using interleaved presentations of a shock-predictive tone (paired conditioned stimulus, CS+) that terminated with a footshock (unconditioned stimulus, US) and a safety-predictive tone that predicted the absence of the footshock (CS−) within a session (Fig. 1a). The box-only control group was placed in the training context but was not exposed to either CS+ or CS− whereas the unpaired training group was exposed to all three stimuli (CS+, CS− and US) in scrambled order, precluding any tone–shock contingency (Extended Data Fig. 1a). Compared to the unpaired group, mice in the paired training group learned the CS+–US association during training, showing an escalation of freezing responses to successive CS presentations (Extended Data Fig. 1b–d) even though both groups increased their freezing behaviour after the tone (Extended Data Fig. 1e). When the mice were tested for long-term memory (LTM), paired training resulted in mice exhibiting a high freezing response to the CS+ while suppressing the response to CS− (Fig. 1b, c), with a robust discrimination index outcome compared to box-only and unpaired controls (Fig. 1d, Extended Data Fig. 1f). Notably, the freezing response

[1]Center for Neural Science, New York University, New York, NY, USA. [2]Department of Biochemistry, McGill University, Montreal, Quebec, Canada. [3]Laboratory of Molecular Biology, The Rockefeller University, New York, NY, USA. [4]NYU Neuroscience Institute, New York University School of Medicine, New York, NY, USA. ✉e-mail: ps755@nyu.edu; eklann@cns.nyu.edu

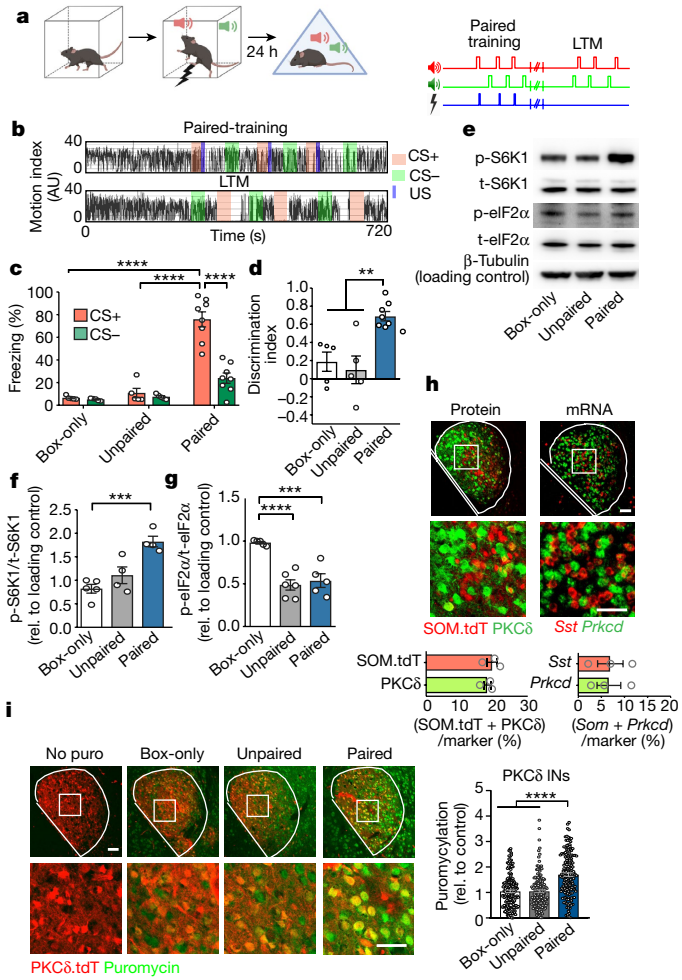

Fig. 1 | Differential threat-conditioning promotes de novo translation in CeL INs. a, Behaviour scheme for differential cued threat conditioning (left) and tone–shock presentation schedule for the paired training group (right). **b**, Representative motion traces for the paired group during training and LTM test. Shaded bars show timing of stimuli. AU, arbitrary units. **c**, During LTM, the paired group showed a stronger freezing response to CS+ than the box-only and unpaired groups. Effect of training: $F(2,30) = 60.08$, $P < 0.0001$; effect of CS, $F(1,30) = 22.86$, $P < 0.0001$. **d**, The paired group showed a high discrimination index for cued threat compared to controls. $F(2,15) = 12.01$, $P = 0.0008$. **c**, **d**, $n = 5$ (box-only), 5 (unpaired) and 8 (paired) mice. **e**, Representative immunoblots for mTORC1 and eIF2 pathway indicators: p-S6K1 (T389), total (t)-S6K1, p-eIF2α (S51), t-eIF2α and β-tubulin. **f**, p-S6K1 (T389) was elevated in amygdala lysate of the paired group compared to the box-only controls. $F(2,10) = 16.41$, $P = 0.0007$. $n = 5$ (box-only), 4 (unpaired) and 4 (paired) mice. Rel., relative. **g**, Dephosphorylation of eIF2α (S51) occurred in both unpaired and paired groups (right). $F(2,13) = 20.94$, $P < 0.0001$. $n = 5$ (box-only), 6 (unpaired) and 5 (paired) mice. **h**, Left, immunostaining for PKCδ in SOM.tdT mice revealed largely distinct cell populations; 18.06% of PKCδ$^+$ neurons co-expressed SOM.tdT whereas 19.56% of SOM.tdT neurons co-expressed PKCδ. Right, single-molecule fluorescent in situ hybridization (smFISH) for *Prkcd* and *Sst* mRNA shows that double-positive cells constitute 6.63% of *Prkcd*$^+$ cells and 6.94% of *Sst*$^+$ cells. $n = 3$ mice per group. **i**, De novo translation was upregulated in PKCδ INs in the paired training group compared to controls. $F(2,482) = 44.18$, $P < 0.0001$. $n = 162$ (box-only), 158 (unpaired) and 165 (paired) cells from three mice per group. Puro, puromycin. **c**, Two-way ANOVA with Bonferroni's post-hoc test; **c**, **f**, **g**, **i**, one-way ANOVA with Bonferroni's post hoc test. Mean ± s.e.m. $^*P < 0.05$, $^{**}P < 0.01$, $^{***}P < 0.001$, $^{****}P < 0.0001$. Scale bars, 50 µm.

to CS− was higher than the negligible freezing behaviour during the pre-CS period (Extended Data Fig. 1g, h). An increase in the number of CS+–US pairings from three to five increased freezing with successive CS presentations during memory acquisition (Extended Data Fig. 1i, j), but did not improve the freezing response to either the CS+ and CS− or the discrimination index during LTM testing (Extended Data Fig. 1k, l), indicating that the learned behaviour had reached an asymptote after three pairings. Biochemical analysis of the amygdala showed that activation of mTORC1, as indicated by phosphorylation of S6K1, occurs in the paired group but not in the box-only or unpaired groups (Fig. 1e, f). Notably, dephosphorylation of eIF2α occurred in both the paired and unpaired groups, indicating that different pathways control translation programs associated with capturing the shock experience versus tone–shock contingencies (Fig. 1e, g). We next focused on populations of inhibitory neurons (INs) that expressed somatostatin (SOM) or protein kinase Cδ (PKCδ)[17–19], each of which constitutes approximately half of all neurons in the centrolateral amygdala (CeL) (Extended Data Fig. 2a, b) and are largely distinct (Fig. 1h, Extended Data Fig. 2c–e). The phosphorylation of ribosomal protein S6 at Ser 235/236 was increased in both SOM and PKCδ INs in the paired group compared to the box-only and unpaired groups, indicating that differential threat conditioning activated the mTORC1 pathway (Extended Data Fig. 2f, g). We then used in vivo surface sensing of translation (SUnSET) to label newly synthesized proteins with the synthetic tyrosyl-tRNA analogue puromycin in awake behaving mice. De novo translation in the CeL, specifically in PKCδ INs, was increased in the paired group compared to both unpaired and box-only controls (Fig. 1h, Extended Data Fig. 3a, b).

To test whether cap-dependent translation in CeL INs has a causal role in the formation of differential threat memories, we devised an intersectional chemogenetic strategy to stably knock down eIF4E in SOM and PKCδ INs for a defined period. We used knock-in mouse-based conditional expression of a synthetic micro-RNA that specifically targets *Eif4e* mRNA[20], consisting of *Eif4e*-specific short hairpin RNA (shRNA) embedded in the miRNA-30 backbone (shmiR; Fig. 2a). shmiRs are driven by Pol II promoters and act as natural substrates in miRNA biogenesis pathways, leading to the robust expression of mature shRNA and high knockdown efficiency[21]. The shmiR for *Eif4e* (shmiR-4E) is integrated in the 3′ untranslated region (UTR) of GFP and is under transcriptional regulation by tet-responsive elements (TREs). In double-transgenic *Sst-cre::TRE-GFP.shmiR-4E* and *Prckd-cre:TRE-GFP.shmiR-4E* mice (in which eIF4E is knocked down in SOM or PKCδ INs), we virally expressed the Cre-dependent tet transactivator (tTA) in the CeL while placing the animals on a diet lacking doxycycline for 14 days following viral delivery to mediate knockdown of eIF4E (4Ekd) (Fig. 2b, Extended Data Fig. 4a, b). This strategy resulted in a substantial reduction in eIF4E protein (Extended Data Fig. 4c, d) and, subsequently, in inhibition of de novo global translation in CeL INs compared to GFP controls (Extended Data Fig. 4e, f). MMP9, the protein product of an eIF4E-sensitive mRNA that is important for long-lasting synaptic plasticity in the central amygdala[22], was also substantially reduced in SOM and PKCδ INs (Extended Data Fig. 4g, h). At the level of behaviour, eIF4E knockdown in SOM INs did not affect spontaneous locomotion in the open field and elevated plus maze (Extended Data Fig. 5a–h). However, mice lacking eIF4E in PKCδ INs (PKCδ.4Ekd mice), despite exhibiting normal open field activity (Extended Data Fig. 5i–m), explored the open arm of an elevated plus maze more than control mice, indicating reduced anxiety (Extended Data Fig. 5n–p). A reduction in anxiety induced by inhibition of cap-dependent translation in PKCδ INs is consistent with the previous finding that optogenetic silencing of PKCδ neurons in the CeL decreases anxiety[23].

To test whether inhibition of cap-dependent translation in CeL IN subtypes has any effect on long-term threat memory, we trained SOM.4Ekd and PKCδ.4Ekd mice in a simple cued threat-conditioning paradigm in which a tone unambiguously terminated with a footshock (Fig. 2c, Extended Data Fig. 6a). Although all mice learned the CS–US association equivalently (Fig. 2d, Extended Data Fig. 6b), only SOM.4Ekd mice showed a significant deficit in LTM (Fig. 2e, Extended Data Fig. 6c). SOM.4Ekd mice that were fed a diet including doxycycline for 14 days (to allow the expression of eIF4E) and then re-trained in the same protocol

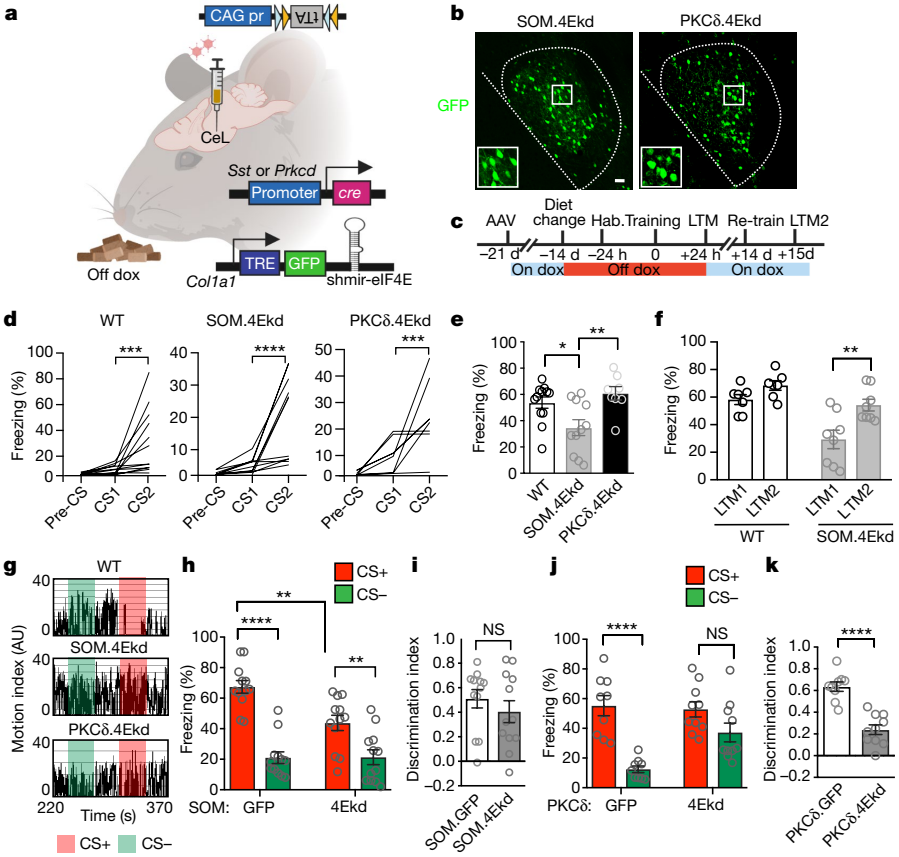

Fig. 2 | Cell type-specific inhibition of cap-dependent translation in CeL INs. a, Intersectional chemogenetic strategy for knocking down eIF4E in CeL INs. pr, promoter. **b**, Brain-region- and cell-type-specific expression of GFP. shmir-eIF4E in CeL SOM and PKCδ INs. **c**, Behaviour paradigm for simple and differential cued threat-conditioning. Hab., habituation. **d**, Normal memory acquisition for simple threat conditioning in wild-type (WT), SOM.4Ekd and PKCδ.4Ekd groups. WT, $F(2,33) = 10.44$, $P = 0.0003$; SOM.4Ekd, $F(2,30) = 16.26$, $P < 0.0001$; PKCδ.4Ekd, $F(2,21) = 13.46$, $P = 0.0002$. **e**, SOM.4Ekd mice display significantly impaired LTM compared to wild-type or PKCδ.4Ekd mice. $F(2,28) = 6.41$, $P = 0.0051$. **d**, **e**, $n = 12$ (WT), 11 (SOM.4Ekd) and 8 (PKCδ.4Ekd) mice. **f**, Re-training SOM.4Ekd mice after placing on doxycycline (dox)-containing diet for 14 days rescued the memory deficit. Effect of drug, $F(1,13) = 12.33$, $P = 0.0038$; effect of genotype, $F(1,13) = 21.13$, $P = 0.0005$. $n = 7$ (WT) and 8 (SOM.4Ekd) mice. **g**, Representative motion traces during differential threat LTM test. **h**, SOM.4Ekd mice are impaired in CS+ threat LTM compared to SOM.GFP controls, but show equivalent safety response to CS−. Effect of genotype, $F(1,44) = 6.68$, $P = 0.013$; effect of CS, $F(1,44) = 58.41$, $P < 0.0001$. $n = 12$ mice per group. **i**, Normal cue discrimination index for SOM.4Ekd mice compared to controls. $P = 0.377$. **j**, PKCδ.4Ekd mice are impaired in safety LTM to CS− despite showing normal threat LTM to CS+. Effect of genotype, $F(1,34) = 4.17$, $P = 0.049$; effect of CS, $F(1,34) = 28.60$, $P < 0.0001$. $n = 9$ (PKCδ.GFP) and 10 (PKCδ.4Ekd) mice. **k**, Discrimination index for cued threat is impaired in PKCδ.4Ekd mice. $P < 0.0001$. $n = 9$ (PKCδ.GFP) and 10 (PKCδ.4Ekd) mice. **d**, **f**, Repeated measures one-way ANOVA with Bonferroni's post-hoc test; **e**, one-way ANOVA with Bonferroni's post-hoc test; **h**, **j**, two-way ANOVA with Bonferroni's post-hoc test; **i**, **k**, unpaired *t*-test, two-tailed. Mean ± s.e.m. $^*P < 0.05$, $^{**}P < 0.01$, $^{***}P < 0.001$, $^{****}P < 0.0001$. NS, nonsignificant. Scale bar, 50 µm.

showed complete rescue of LTM (Fig. 2f). Next, we tested 4Ekd animals in the differential threat-conditioning paradigm (Fig. 1a). SOM.4Ekd mice learned equivalently to SOM.GFP mice (Extended Data Fig. 6d–f). During LTM, SOM.4Ekd mice displayed a selective impairment in the conditioned-threat response to the CS+ but showed a normal safety response to CS− and a normal cue discrimination index (Fig. 2g–i). PKCδ.4Ekd mice also acquired differential threat associative memory normally (Extended Data Fig. 6g–i). However, PKCδ.4Ekd mice showed a selective impairment in the conditioned-safety response to CS−, despite a normal conditioned-threat response to CS+ (Fig. 2g, j), which led to a sub-optimal cue discrimination index for PKCδ.4Ekd animals (Fig. 2k). Both SOM.4Ekd and PKCδ.4Ekd animals displayed negligible baseline freezing during pre-CS (Extended Data Fig. 6j–m). Overall, these results show that prevention of cap-dependent translation in SOM and PKCδ INs results in selective impairments in conditioned threat and safety responses, respectively.

To understand the contribution of time-limited de novo protein synthesis during the initial consolidation window following learning, we applied a knock-in mouse-based chemogenetic strategy[10] to express Cre-dependent and drug-inducible double-stranded RNA-activated protein kinase (iPKR) in SOM and PKCδ INs (Fig. 3a). Because the iPKR mouse line also enables Cre-dependent expression of eGFP-tagged ribosomal subunit L10, we detected soma-localized GFP in the CeL SOM and PKCδ neurons of SOM.iPKR and PKCδ.iPKR mice, respectively (Fig. 3b). In vivo infusion of Asunaprevir (ASV), the drug inducer of iPKR, substantially increased the phosphorylation of eIF2α (S51) in SOM and PKCδ INs in the CeL (Extended Data Fig. 7a, b). We then exposed the animals to the differential threat-conditioning paradigm as described above, but restricted cell-type-specific inhibition of protein synthesis to the initial consolidation period by infusing ASV into the CeL immediately after training (Fig. 3c). Although all mice learned equivalently during training (Extended Data Fig. 7c–h), we found remarkably divergent memory deficits in SOM.iPKR and PKCδ.iPKR mice. Similar to the 4Ekd approach, we found that blocking general translation with increased eIF2α phosphorylation in SOM INs impaired the freezing response to CS+ while keeping the safety response and cue discrimination intact (Fig. 3d–f). On the other hand, blocking general translation with increased eIF2α phosphorylation in PKCδ INs resulted in an

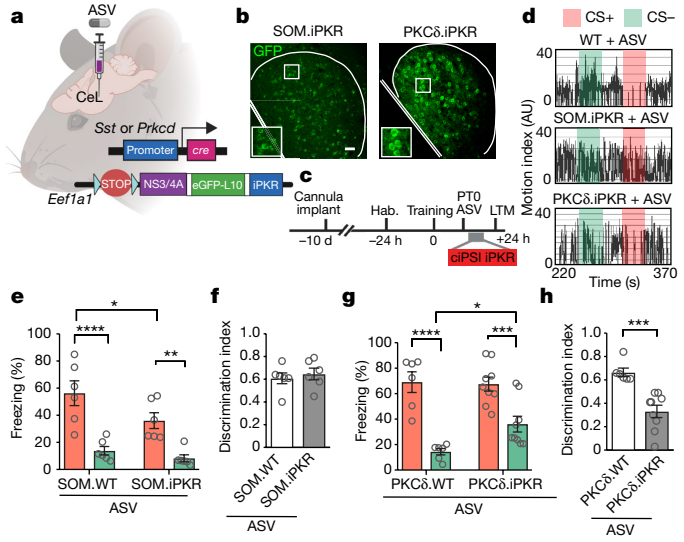

Fig. 3 | Blocking eIF2-dependent translation in specific CeL INs impairs consolidation of differential threat memories. a, Chemogenetic strategy for drug-inducible, cell-type-specific phosphorylation of eIF2α in SOM and PKCδ INs in CeL. **b**, eGFP–L10 expression in SOM.iPKR and PKCδ.iPKR CeL INs. **c**, Behaviour paradigm for differential cued threat conditioning with temporally precise inhibition of protein synthesis during initial consolidation. **d**, Representative LTM motion traces for WT + ASV, SOM.iPKR + ASV and PKCδ.iPKR + ASV mice. **e**, Intra-CeL infusion of ASV decreased threat response to CS+ in SOM.iPKR mice while sparing the conditioned safety response to CS−. Effect of genotype, $F(1,20) = 4.90$, $P = 0.0376$; effect of CS, $F(1,20) = 36.78$, $P < 0.0001$. $n = 6$ mice per group. **f**, Normal discrimination index for cued threat in SOM WT and SOM.iPKR mice. $P = 0.595$. $n = 6$ mice per group. **g**, Intra-CeL infusion of ASV in PKCδ.iPKR mice did not affect the threat response to CS+ but impaired the safety response to CS−. Effect of CS, $F(1,26) = 48.85$, $P < 0.0001$. **h**, Discrimination index for cued threat was impaired in PKCδ.iPKR + ASV animals compared to controls. $P = 0.0005$. **g**, **h**, $n = 6$ (PKCδ.WT + ASV) and 9 (PKCδ.iPKR + ASV) mice. **e**, **g**, Two-way ANOVA with Bonferroni's post-hoc test; **f**, **h**, unpaired *t*-test. Mean ± s.e.m. $^*P < 0.05$, $^{**}P < 0.01$, $^{***}P < 0.001$, $^{****}P < 0.0001$. Scale bar, 50 µm.

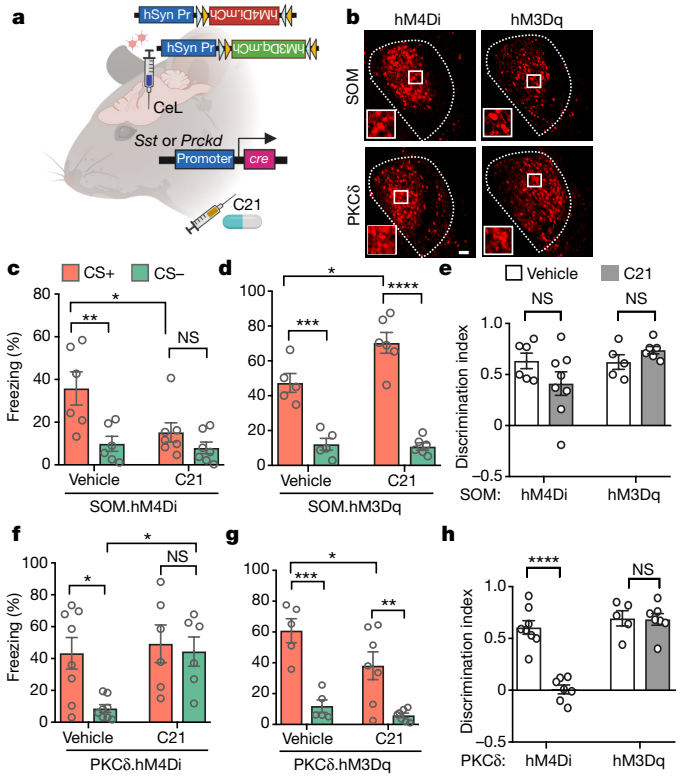

Fig. 4 | Conserved G-protein-signalling pathways in CeL INs modulate threat and safety responses. a, Chemogenetic strategy for expressing designer $G_{\alpha i}$ (hM4Di) or $G_{\alpha q}$ (hM3Dq) protein-coupled DREADD receptors in CeL SOM and PKCδ INs. **b**, Representative immunohistochemical images for mCherry fused to DREADD receptors in CeL SOM and PKCδ INs. **c**, Conditioned threat response to CS+ is impaired for SOM.hM4Di + C21 group compared to vehicle controls. Effect of drug, $F(1,22) = 5.39$, $P = 0.0299$; effect of CS, $F(1,22) = 11.76$, $P = 0.0024$. $n = 6$ (vehicle) and 7 (C21) mice. **d**, Conditioned threat response to CS+ is increased in SOM.hM3Dq + C21 group compared with vehicle controls. $F(1,18) = 5.703$, $P = 0.0281$. $n = 5$ (vehicle) and 6 (C21) mice. **e**, Discrimination index for cued threat is normal across all SOM groups. Effect of genotype, $F(1,21) = 3.015$, $P = 0.097$; effect of drug, $F(1,21) = 0.338$, $P = 0.561$. SOM.hM4Di, $n = 6$ (vehicle) and 8 (C21) mice. SOM.hM3Dq: $n = 5$ (vehicle) and 6 (C21) mice. **f**, Conditioned safety response to CS− is impaired in PKCδ.hM4Di mice given C21 compared to vehicle controls. Effect of drug, $F(1,24) = 5.702$, $P = 0.0252$; effect of CS, $F(1,24) = 5.119$, $P = 0.0330$. $n = 8$ (vehicle) and 6 (C21) mice. **g**, Conditioned threat response to CS+ is reduced in PKCδ.hM3Dq mice given C21 compared to vehicle controls. Effect of drug, $F(1,20) = 4.77$, $P = 0.041$; effect of CS, $F(1,20) = 38.02$, $P < 0.0001$. $n = 5$ (vehicle) and 7 (C21) mice. **h**, Discrimination index for cued threat is impaired for PKCδ.hM4Di + C21 mice compared to controls but unaltered for other groups. Effect of genotype, $F(1,23) = 39.15$, $P < 0.0001$; effect of drug, $F(1,23) = 24.78$, $P < 0.0001$. PKCδ.hM4Di: $n = 8$ (vehicle) and 7 (C21) mice; PKCδ.hM3Dq: $n = 5$ (vehicle) and 7 (C21) mice. **c**–**h**, Two-way ANOVA with Bonferroni's post-hoc test. Mean ± s.e.m. $^*P < 0.05$, $^{**}P < 0.01$, $^{***}P < 0.001$, $^{****}P < 0.0001$. NS, nonsignificant. Scale bar, 50 µm.

impaired safety response and cue discrimination, with no reduction in freezing response to CS+ during LTM (Fig. 3d, g, h). Thus, the simultaneous consolidation of long-lasting threat and safety responses requires de novo protein synthesis in distinct populations of INs in the CeL.

Protein synthesis machinery within neurons is modulated by events at the cell membrane that communicate trans-synaptic inputs via intracellular signalling cascades. We therefore examined the conserved cell-autonomous $G_{\alpha i}$- and $G_{\alpha q}$-protein signalling pathways in CeL INs using viral expression of designer receptors activated by designer drugs (DREADDs) that are based on mutant muscarinic acetylcholine receptors and couple to G proteins[24] (Fig. 4a, b). Specifically, $G_{\alpha i}$-protein signalling (mediated by the hM4Di designer receptor) leads to inhibition of adenylyl cyclase and decreases neuronal activity, whereas $G_{\alpha q}$-protein signalling (mediated by the hM3Dq designer receptor) results in activation of phospholipase C and can boost de novo translation[10,24]. In the differential threat-conditioning paradigm, pre-training administration of the DREADD agonist C21 did not alter learning in SOM.tdT, SOM.hM4Di or SOM.hM3Dq mice (Extended Data Fig. 8a–i). During memory retrieval, C21 had opposing behavioural effects on SOM.hM4Di and SOM.hM3Dq mice, and had no effect on control SOM.tdT animals (Extended Data Fig. 8j, k). C21 treatment substantially decreased the conditioned-threat response to CS+ in SOM.hM4Di mice (Fig. 4c). This threat-response deficit, caused by activating $G_{\alpha i}$-protein signalling in SOM INs, is consistent with the behavioural effects of inhibition of de novo translation in these CeL INs. By contrast, increasing neuronal activity in SOM INs by activating the $G_{\alpha q}$-protein pathway during threat-conditioning resulted in enhanced LTM for the CS+ (Fig. 4d). These findings support the idea that chemogenetic manipulation of conserved G-protein signalling in SOM INs results in bidirectional modulation of the threat response, consistent with previous findings[1,3]. C21 did not alter the cued threat discrimination index (Fig. 4e) or baseline freezing during the pre-CS phase of either the memory acquisition or retrieval phase (Extended Data Fig. 8l, m). Likewise, DREADD manipulation of PKCδ INs did not alter associative learning in PKCδ.tdT, PKCδ.hM4Di or PKCδ.hM3Dq mice (Extended Data Fig. 9a–i). Notably, activation of the $G_{\alpha i}$-protein signalling pathway in PKCδ INs in PKCδ.hM4Di mice given C21 led to a selective impairment in safety response to CS− and in cue discrimination (Fig. 4f, h), whereas activation of the $G_{\alpha q}$-protein signalling pathway in PKCδ INs reduced the threat response to CS+ (Fig. 4g, h). C21 had no effect on memory

retrieval in PKCδ.tdT mice (Extended Data Fig. 9j, k) or on baseline freezing during the pre-CS phases of memory acquisition or retrieval (Extended Data Fig. 9 l, m). These data indicate that $G_{\alpha i}$-protein signalling mirrors the effect of blocking de novo protein synthesis in PKCδ INs. On the other hand, activation of the $G_{\alpha q}$-protein pathway in CeL SOM and PKCδ INs has opposing effects on the CS+ threat response but does not alter the CS− safety response.

Previous studies have reported that long-term spatial and threat memories can be enhanced by relieving translation repression with constitutive deletion of genes that encode eIF2α kinases such as GCN2 and PKR[25,26] or by administering ISRIB, which activates eIF2B[15]. Likewise, constitutive deletion of the gene that encodes the eIF4E repressor 4E-BP2 results in enhanced conditioned taste aversion memory[27] whereas acute intra-amygdalar infusion of 4EGI-1, an inhibitor of the eIF4E–eIF4G interaction, blocks threat memory consolidation[28]. In both simple and differential threat-conditioning paradigms, our results show that eIF2- and eIF4E-dependent translation programs in CeL SOM INs are required for the conditioned-threat response, which indicates that SOM INs are the primary CeL locus for storage of cued threat memory. Our findings are consistent with studies showing long-lasting synaptic potentiation in CeL SOM INs following threat learning that lasts at least 24 h[17]. Moreover, the expression of biallelic phosphomutant eIF2α in SOM INs brainwide results in enhanced cued and contextual LTM[29]. In a contrasting but complementary role, de novo translation in PKCδ INs serves to store the conditioned-safety response. Our findings thus support a working model in which CeL SOM and PKCδ INs simultaneously store threat and safety cue-associated memories, respectively, by changing the cellular translation landscape (Extended Data Fig. 10).

Threat generalization resulting from an impaired safety response is a hallmark feature of post-traumatic stress disorder (PTSD)[5]. In auditory threat conditioning, overtraining or increasing the US intensity has been shown to increase auditory threat generalization[30]. Cells in the lateral amygdala shift the threat response from cue-specific to cue-generalization depending on the intensity of the US[31]. Within the CeL, PKCδ INs are direct recipients of US-related nociceptive input from the parabrachial nucleus[8]. Our demonstration here that blocking neuronal activity and de novo protein synthesis in CeL PKCδ INs disrupts the acquisition and consolidation of long-term inhibition of the conditioned response to the non-reinforced tone (CS−) is in agreement with the US-processing feature of these types of neuron. To our knowledge, our study provides the first evidence that the disruption of protein synthesis in discrete IN subpopulations in the CeL impairs associative memories related to threat and safety, which may contribute to maladaptive behaviour in memory disorders such as PTSD.

Online content

Any methods, additional references, Nature Research reporting summaries, source data, extended data, supplementary information, acknowledgements, peer review information; details of author contributions and competing interests; and statements of data and code availability are available at https://doi.org/10.1038/s41586-020-2793-8.

1. Fendt, M. & Fanselow, M. S. The neuroanatomical and neurochemical basis of conditioned fear. *Neurosci. Biobehav. Rev.* **23**, 743–760 (1999).
2. Pavlov, I. P. *Conditioned Reflexes: an Investigation of the Physiological Activity of the Cerebral Cortex* (Oxford Univ. Press, 1927)
3. Rescorla, R. A. Pavlovian conditioned inhibition. *Psychol. Bull.* **72**, 77–94 (1969).
4. Christianson, J. P. et al. Inhibition of fear by learned safety signals: a mini-symposium review. *J. Neurosci.* **32**, 14118–14124 (2012).
5. Jovanovic, T. et al. Impaired fear inhibition is a biomarker of PTSD but not depression. *Depress. Anxiety* **27**, 244–251 (2010).
6. Wilensky, A. E., Schafe, G. E., Kristensen, M. P. & LeDoux, J. E. Rethinking the fear circuit: the central nucleus of the amygdala is required for the acquisition, consolidation, and expression of Pavlovian fear conditioning. *J. Neurosci.* **26**, 12387–12396 (2006).
7. Ciocchi, S. et al. Encoding of conditioned fear in central amygdala inhibitory circuits. *Nature* **468**, 277–282 (2010).
8. Han, S., Soleiman, M. T., Soden, M. E., Zweifel, L. S. & Palmiter, R. D. Elucidating an affective pain circuit that creates a threat memory. *Cell* **162**, 363–374 (2015).
9. Haubensak, W. et al. Genetic dissection of an amygdala microcircuit that gates conditioned fear. *Nature* **468**, 270–276 (2010).
10. Shrestha, P. et al. Cell-type-specific drug-inducible protein synthesis inhibition demonstrates that memory consolidation requires rapid neuronal translation. *Nat. Neurosci.* **23**, 281–292 (2020).
11. Kandel, E. R., Dudai, Y. & Mayford, M. R. The molecular and systems biology of memory. *Cell* **157**, 163–186 (2014).
12. Klann, E. & Dever, T. E. Biochemical mechanisms for translational regulation in synaptic plasticity. *Nat. Rev. Neurosci.* **5**, 931–942 (2004).
13. Costa-Mattioli, M. et al. eIF2α phosphorylation bidirectionally regulates the switch from short- to long-term synaptic plasticity and memory. *Cell* **129**, 195–206 (2007).
14. Kats, I. R. & Klann, E. Translating from cancer to the brain: regulation of protein synthesis by eIF4F. *Learn. Mem.* **26**, 332–342 (2019).
15. Sidrauski, C., McGeachy, A. M., Ingolia, N. T. & Walter, P. The small molecule ISRIB reverses the effects of eIF2α phosphorylation on translation and stress granule assembly. *eLife* **4**, e05033 (2015).
16. Thoreen, C. C. et al. A unifying model for mTORC1-mediated regulation of mRNA translation. *Nature* **485**, 109–113 (2012).
17. Li, H. et al. Experience-dependent modification of a central amygdala fear circuit. *Nat. Neurosci.* **16**, 332–339 (2013).
18. Fadok, J. P. et al. A competitive inhibitory circuit for selection of active and passive fear responses. *Nature* **542**, 96–100 (2017).
19. Yu, K., Garcia da Silva, P., Albeanu, D. F. & Li, B. Central amygdala somatostatin neurons gate passive and active defensive behaviors. *J. Neurosci.* **36**, 6488–6496 (2016).
20. Lin, C.-J. et al. Targeting synthetic lethal interactions between Myc and the eIF4F complex impedes tumorigenesis. *Cell Rep.* **1**, 325–333 (2012).
21. Dickins, R. A. et al. Probing tumor phenotypes using stable and regulated synthetic microRNA precursors. *Nat. Genet.* **37**, 1289–1295 (2005).
22. Gorkiewicz, T., Balcerzyk, M., Kaczmarek, L. & Knapska, E. Matrix metalloproteinase 9 (MMP-9) is indispensable for long term potentiation in the central and basal but not in the lateral nucleus of the amygdala. *Front. Cell. Neurosci.* **9**, 73 (2015).
23. Botta, P. et al. Regulating anxiety with extrasynaptic inhibition. *Nat. Neurosci.* **18**, 1493–1500 (2015).
24. Guettier, J.-M. et al. A chemical-genetic approach to study G protein regulation of beta cell function in vivo. *Proc. Natl Acad. Sci. USA* **106**, 19197–19202 (2009).
25. Costa-Mattioli, M. et al. Translational control of hippocampal synaptic plasticity and memory by the eIF2α kinase GCN2. *Nature* **436**, 1166–1173 (2005).
26. Zhu, P. J. et al. Suppression of PKR promotes network excitability and enhanced cognition by interferon-γ-mediated disinhibition. *Cell* **147**, 1384–1396 (2011).
27. Banko, J. L. et al. Behavioral alterations in mice lacking the translation repressor 4E-BP2. *Neurobiol. Learn. Mem.* **87**, 248–256 (2007).
28. Hoeffer, C. A. et al. Inhibition of the interactions between eukaryotic initiation factors 4E and 4G impairs long-term associative memory consolidation but not reconsolidation. *Proc. Natl Acad. Sci. USA* **108**, 3383–3388 (2011).
29. Sharma, V. et al. eIF2α controls memory consolidation via excitatory and somatostatin neurons. *Nature* https://doi.org/10.1038/s41586-020-2805-8 (2020).
30. Laxmi, T. R., Stork, O. & Pape, H.-C. Generalization of conditioned fear and its behavioral expression in mice. *Behav. Brain Res.* **145**, 89–98 (2003).
31. Ghosh, S. & Chattarji, S. Neuronal encoding of the switch from specific to generalized fear. *Nat. Neurosci.* **18**, 112–120 (2015).

Methods

Animals

All animal protocols were reviewed and approved by the New York University Animal Care and Use Committee. Mice were provided with food and water ad libitum and were maintained in a 12 h–12 h light–dark cycle at New York University at a stable temperature (78 °F) and humidity (40–50%). All mice were backcrossed to C57Bl/6J strain for at least five generations. Both male and female mice, aged 3–6 months, were used in all experiments. Somatostatin IRES-Cre knockin mice (SOM-Cre; stock 013044) were obtained from Jackson labs. PKCδ:: GluClα-iCre BAC transgenic mice (PKCδ-Cre)[9] were generated by GENSAT and kindly provided by Dr. David Anderson (Caltech). Cre reporter lines including floxed TRAP (stock 022367) mice expressing GFP–L10 fusion protein in a Cre-dependent manner, and floxed tdTomato mice (Ai14; stock 007908) that express tdTomato in a Cre-dependent manner, were obtained from Jackson labs. Col1a1$^{TRE\,GFP.shmiR\text{-}4E.389}$ mice were generated as previously described[26]. Floxed iPKR (Eef1a1$^{LSL.NS3/4.TRAP.iPKR}$) mice were generated as previously described[10]. SOM-Cre and PKCδ-Cre mice were crossed with floxed Col1a1$^{TRE\,GFP.shmiR\text{-}4E}$ mice to generate transheterozygote SOM-Cre::TRE-GFP.shmiR-4E and PKCδ-Cre::TRE-GFP.shmiR-4E mice, respectively. Likewise, SOM-Cre and PKCδ-Cre mice were crossed with floxed iPKR mice to generate transheterozygote SOM.iPKR and PKCδ.iPKR mice, respectively. SOM.tdT and PKCδ.tdT mice were generated by crossing SOM-Cre and PKCδ-Cre with the floxed tdTomato reporter line, whereas PKCδ.TRAP mice were generated by crossing PKCδ-Cre line with floxed TRAP mice. SOM.tdT.TRE-GFP.shmiR-eIF4E and PKCδ.tdT.TRE-GFP.shmiR-eIF4E mice were generated by breeding SOM-Cre::TRE-GFP.shmiR-4E and PKCδ-Cre::TRE-GFP.shmiR-4E mice with the homozygous floxed tdTomato reporter line. Wild-type C57Bl/6J mice (stock 000664) were purchased from Jackson labs.

Drugs and chemicals

Doxycycline was added to rodent chow at 40 mg/kg (Bio-Serv, F4159). This doxycycline diet was provided to SOM.4Ekd, PKCδ.4Ekd, and control SOM.WT and PKCδ.WT mice starting from the day of surgery for 7 d and to the SOM.4Ekd re-training group for 14 d after LTM1 ad libitum. ASV (ChemExpress) was dissolved in DMSO to a stock concentration of 10 mM and diluted in sterile saline to 100 nM. A volume of 0.5 µl was intracranially infused into the CeL (−1.22 mm AP, ±3.00 mm ML, −4.60 mm DV) of SOM.iPKR and PKCδ.iPKR mice using an injection cannula inserted into a stainless-steel guide cannula (Plastics One). ASV infusion was carried out at 0.125 µl/min using an injection cannula extending out of PE50 tubing attached to a 5 µl Hamilton syringe (Hamilton) using a PHD 2000 Infusion Pump (Harvard Apparatus). After injection, the injection cannula was kept in place for 1 min before its withdrawal. Puromycin (Sigma, P8833) was dissolved in ddH_2O at 25 µg/µl, and this stock was freshly diluted in saline to 10 µg/µl for SUnSET assays in vivo. Digitonin (Sigma, D141) was dissolved in ddH_2O at 5% w/v to prepare the stock solution, which was diluted to 0.0015% w/v in 0.1 M PBS. Stock solution of aqueous 32% paraformaldehyde (EMS, 15714) was freshly diluted to 4% in 0.1 M PBS for transcardial perfusions and post-fixation of brain slices. The DREADD actuator, agonist C21 (Tocris 5548), was dissolved in DMSO at 40 mg ml^{-1} concentration, freshly diluted in saline and administered to mice at 1 mg/kg intraperitoneally.

Stereotaxic surgeries

Mice were anaesthetized with the mixture of ketamine (100 mg/kg) and xylazine (10 mg/kg) in sterile saline (i.p. injection). Stereotaxic surgeries were carried out using a Kopf stereotaxic instrument (model 942), which was equipped with a microinjection unit (model 5000). Viral vectors were injected intracranially using a 2.0 µl Neuros syringe (Hamilton, 65459-02). Postoperative analgesia was delivered using subcutaneous injections of ketoprofen (3 mg/kg) for 3 days starting from the day of surgery. To generate SOM.4Ekd and PKCδ.4Ekd mice, 300 nl of AAV9.CAG Pr.DIO.tTA (1.0×10^{13} GC/ml; Vigene) was injected into the CeL (−1.22 mm AP, ±3.00 mm ML and −4.60 mm DV) of double transheterozygote SOM-Cre::TRE-GFP.shmiR-4E and PKCδ-Cre::TRE-GFP.shmiR-4E mice. The plasmid encoding tet transactivator in a Cre-selective manner and under the transcriptional control of CAG promoter (pAAV.CAG Pr.DIO.tTA) was kindly provided by Hongkui Zeng (Allen Institute for Brain Science). For DREADD experiments, SOM-Cre and PKCδ-Cre mice were injected with 300 nl AAV8.hSyn Pr.DIO.hM3Dq-mCherry ($\geq 4 \times 10^{12}$ viral genomes (vg)/ml; Addgene 44361-AAV8) or AAV9.hSyn Pr.DIO.hM4Di-mCherry ($\geq 1 \times 10^{13}$ vg/ml, Addgene 44362-AAV9). For controls, wild-type SOM and PKCδ mice were injected into the CeL with 100 nl AAV9.CAG Pr.DIO.GFP (3.33×10^{13} GC/ml, Penn Vector Core CS1171) to generate SOM.GFP and PKCδ.GFP mice. Behaviour and histology experiments for all viral vector-injected animals were carried out 2–3 weeks after surgery. A cohort of SOM.iPKR and PKCδ.iPKR mice were injected bilaterally in CeL with 200 nl AAV.Eef1a1 Pr.DIO.eGFP-L10a (7×10^{12} GC/ml; Addgene 98747) for immunohistochemistry experiments. Intracranial cannula implant surgeries were carried out using custom-designed guide cannulas (Plastics One) along with a skull screw (1.6 mm shaft) to stabilize the dental cement, Metabond quick adhesive cement (Parkell S380), encapsulating the skull surface. For in vivo surface labelling of translation (SUnSET), SOM.4Ekd, PKCδ.4Ekd and control mice were implanted with a 23-gauge stainless steel guide cannula in the right CeL (−1.22 mm AP, +3.00 mm ML and −2.40 mm DV) for puromycin infusion using an internal cannula with 2 mm projection. Similarly, SOM.iPKR and PKCδ.iPKR mice were also implanted with the 23-gauge stainless steel cannulas in CeL bilaterally for ASV infusions.

Behaviour

All behaviour sessions were conducted during the light cycle. Both male and female mice were included in all behaviour experiments. Mice were randomly assigned to experimental conditions including drug or vehicle infusions, and for the order of testing in any given experimental paradigm. All behaviour data were collected by experimenters blind to the genotype and experimental conditions. SOM.4Ekd, PKCδ.4Ekd and control mice were trained in threat-conditioning paradigms after 14 days of eIF4E knockdown (off dox). A separate group of SOM.4Ekd, PKCδ.4Ekd and control mice were tested in the open field arena and elevated plus maze test after the same duration of eIF4E knockdown. SOM.iPKR and PKCδ.iPKR mice were trained in threat-conditioning paradigms 10 days after cannula implant surgeries to allow time for recovery.

Open field activity

Mice were placed in the centre of an open field (27.31 × 27.31 × 20.32 cm) for 15 min during which a computer-operated optical system (Activity monitor software, Med Associates) monitored the spontaneous movement of the mice as they explored the arena. The parameters tested were distance travelled, and the ratio of centre to total time.

Elevated plus maze

The plus maze consisted of two open arms (30 cm × 5 cm) and two enclosed arms of the same size with 14-cm-high sidewalls and an endwall. The arms extended from a common central square (5 cm^2 × 5 cm^2) perpendicular to each other, making the shape of a plus sign. The entire plus-maze apparatus was elevated to a height of 38.5 cm. Testing began by placing a mouse on the central platform of the maze facing the open arm. A standard 5-min test duration was applied, and the maze was wiped with 30% ethanol in between trials. Ethovision XT13 software (Noldus) was used to record the time spent on open arms and closed arms, total distance moved, and number of open arm and closed arm entries.

Simple cued threat conditioning

Mice were habituated for 15 min in the threat-conditioning chambers housed inside sound-attenuated cubicles (Coulbourn Instruments) on

the habituation day. The habituation and training context included a metal grid floor and a white houselight. For simple threat conditioning, mice were placed in the context for 270 s and then presented twice with a 5-kHz, 85-dB pure tone for 30 s that co-terminated with a 2-s, 0.5-mA footshock. The intertrial interval (ITI) was 2 min and after the second tone–shock presentation, mice remained in the chamber for an additional 120 s. Cued threat-conditioning (cTC) LTM was tested 24 h after training, in a novel context (context B: vanilla-scented cellulose bedding, plexiglas platform, and red houselight) with three presentations of the paired tone (conditioned stimulus, CS). Freezing behaviour was automatically measured using Freeze Frame software (ActiMetrics) and manually re-scored and verified by an experimenter blinded to the genotype or drug treatment. Motion traces were generated using the Freeze Frame software.

Differential cued threat conditioning

For standard differential threat conditioning, mice were placed in the training context for 250 s and then trained with interleaved presentations of three paired tones or CS+ (7.5 kHz pulsatile tone, 50% duty cycle) that co-terminated with a 0.5 mA footshock and three unpaired tones or CS− (3 kHz pure tone) in the training context with variable ITI. Specifically, the CS+ (7.5 kHz) was presented at 270, 440 and 570 s and was paired with a footshock, whereas the 3-kHz pure tone occurred at 370, 520 and 660 s. On the next day, cued threat discrimination (cTD) LTM was tested with three interleaved presentations of CS+ and CS− tones with the order reversed from the training day and with variable intertrial intervals. Specifically, the 3-kHz CS− tone was presented at 250, 380 and 550 s, whereas the 7.5-kHz pulsed tone was presented at 310, 450 and 630 s. All tones lasted for 30 s. After the last CS− tone, mice remained in the testing context for an additional 60 s. When specifically stated, the CS− tones were assigned as 1 kHz pure tone. The box-only control group were placed in the training context for the same duration as the cTD (paired) group but they did not receive any footshock or exposure to CS+ or CS−. The unpaired control group were presented with three interleaved presentations of CS+ and CS− like the cTD (paired) group, but the US was presented in between the CSs with no tone–shock contingency. All groups of mice (box-only, paired and unpaired) were tested on the following day with three presentations of CS+ and CS− in reverse sequence compared to the training day. For the paired 5× group, mice were exposed to five presentations of CS+ (7.5-kHz pulsatile tone) that co-terminated with the footshock and five presentations of CS− (3-kHz pure tone) during training and tested with three interleaved presentations of CS+ and CS− during LTM 24 h later.

Freezing behaviour was automatically measured by Freeze Frame software (ActiMetrics) and manually re-scored and verified by an experimenter blinded to genotype or drug treatment. Motion traces were generated using the Freeze Frame software. Discrimination index was calculated as follows:

$$\text{Discrimination index} = \frac{\frac{\sum_{i=1}^{N} \text{CS}+_i}{N} - \frac{\sum_{i=1}^{N} \text{CS}-_i}{N}}{\frac{\sum_{i=1}^{N} \text{CS}+_i}{N} + \frac{\sum_{i=1}^{N} \text{CS}-_i}{N}}$$

where N is the number of animals, CS+ is the freezing response to CS+ (%), and CS− is the freezing response to CS− (%).

Western blot

Mice were killed by cervical dislocation, and 300-µm-thick brain slices containing the amygdala (bregma −1.22 mm to −2.06 mm) were prepared in cold (4 °C) carbooxygenated (95% O_2, 5% CO_2) cutting solution (110 mM sucrose, 60 mM NaCl, 3 mM KCl, 1.25 mM NaH_2PO_4, 28 mM $NaHCO_3$, 5 mM glucose, 0.6 mM ascorbate, 7 mM $MgCl_2$ and 0.5 mM $CaCl_2$) using a VT1200S vibratome (Leica). The amygdala was micro-dissected from the brain slices and sonicated in ice-cold homogenization buffer (10 mM HEPES, 150 mM NaCl, 50 mM NaF, 1 mM EDTA, 1 mM EGTA, 10 mM $Na_4P_2O_7$, 1% Triton X-100, 0.1% SDS and 10% glycerol) that was freshly supplemented with 10 µl each of protease inhibitor (Sigma) and phosphatase inhibitor (Sigma) per ml of homogenization buffer. Protein concentrations were measured using BCA assay (GE Healthcare). Samples were prepared with 5× sample buffer (0.25 M Tris-HCl pH6.8, 10% SDS, 0.05% bromophenol blue, 50% glycerol and 25% β-mercaptoethanol) and heat denatured at 95 °C for 5 min. Forty micrograms of protein per lane was run in pre-cast 4–12% Bis-Tris gels (Invitrogen) and subjected to SDS–PAGE followed by wet gel transfer to PVDF membranes. After blocking in 5% non-fat dry milk in 0.1 M PBS with 0.1% Tween-20 (PBST), membranes were probed overnight at 4 °C using primary antibodies (rabbit anti-p-S6 (S235/236) 1:1,000 (Cell Signaling #4858), rabbit anti-p-S6K1 Thr389 1:500 (Cell Signaling #9205), rabbit anti-S6K1 1:500 (Cell Signaling #2708), rabbit anti-p-eIF2α Ser51 1:300 (Cell Signaling #9721), rabbit eIF2α 1:1,000 (Cell Signaling #9722), mouse anti-β-tubulin 1:5,000 (Sigma #T8328) and mouse anti-β-actin 1:5,000 (Sigma #A5441). After washing three times in 0.1% PBST, membranes were probed with horseradish peroxidase-conjugated secondary IgG (1:5,000) (Millipore #AP307P and #AP308P) for 1 h at room temperature (RT). Signals from membranes were detected with ECL chemiluminescence (Thermo Pierce) using a Protein Simple instrument. Exposures were set to obtain signals at the linear range and then normalized by total protein and quantified via densitometry using ImageJ software.

In vivo surface labelling of translation (SUnSET)

Awake behaving mice with intracranial cannula implants were infused with 5 µg puromycin (0.5 µl, 10 µg/µl) into the central amygdala using a PHD2000 infusion pump and Hamilton 5.0-µl syringe. Mice were returned to the home cage and translation labelling with puromycin was carried out for 1 h. Mice were deeply anaesthetized with a mixture of ketamine (150 mg/kg) and xylazine (15 mg/kg), and transcardially perfused with 0.1 M PBS, 0.0015% digitonin followed by 4% paraformaldehyde (PFA) in PBS. Brains were extracted and post-fixed in 4% PFA for 24 h, followed by immunohistochemistry.

Immunohistochemistry

Mice were deeply anaesthetized with a mixture of ketamine (150 mg/kg) and xylazine (15 mg/kg), and transcardially perfused with 0.1 M PBS followed by 4% paraformaldehyde in PBS. Brains were removed and postfixed in 4% PFA for 24 h. Forty-micrometre free-floating coronal brain sections containing the amygdala were collected using a Leica vibratome (VT1000 s) and stored in 1× PBS containing 0.05% Na-azide at 4 °C. After blocking in 5% normal goat serum in 0.1 M PBS with 0.1% Triton X-100, brain sections were probed overnight with primary antibodies (chicken anti-eGFP (Abcam #ab13970 1:500; for PKCδ.TRAP, SOM.4Ekd and PKCδ 4Ekd brain sections), rabbit anti-eGFP 1:300 (Thermo Fisher #G10362; for SOM.iPKR and PKCδ. iPKR brain sections), rabbit anti-pS6 (S235/6) 1:1,000 (Cell Signaling #4858), rabbit anti-p-eIF2α S51 1:300 (Cell Signaling #9721), rabbit anti-eIF4E 1:500 (Bethyl #A301-153A), rabbit anti-Mmp9 1:300 (Abcam #ab38898), mouse NeuN 1:2,000 (Millipore Sigma #MAB377), chicken anti-somatostatin 1:300 (Synaptic Systems #366 006), rabbit anti-PKCδ 1:250 (Abcam #ab182126), guinea pig anti-RFP 1:500 (Synaptic Systems #390 004), and mouse anti-puromycin 1:1000 (Millipore Sigma #MABE343). After washing three times in 0.1 M PBS, brain sections were incubated with Alexa Fluor conjugated secondary antibodies 1:200 (Abcam #ab175674, #ab175651; Thermo Fisher #A-111034, #A11012, #A21245, #A11073, #A121236, #A21206) in blocking buffer for 1.5 h at RT, and mounted using Prolong Gold antifade mountant with or without DAPI (Life Technologies #P36931, #P36930).

Single-molecule fluorescence in situ hybridization

Mouse brains were collected through flash freezing in OCT Tissue Tek medium (VWR #25608-930) in dry ice. Using a cryostat, each brain

was serially sectioned at 20 µm and thaw-mounted onto Superfrost plus slides spanning AP −1.22 mm to AP −1.70 mm. Slides were stored at −80 °C. smFISH was performed using a RNAscope fluorescent multiplex kit (ACD Bio #320850). *Sst* (#404631-C2) and *Prkcd* (#44191-C3) probes were purchased from the Advanced Cell Diagnostics catalogue. Brain sections were fixed in 4% paraformaldehyde for 15 min and then washed in 50%, 70%, 100% and 100% ethanol for 5 min each. Slides were dried for 10 min and a hydrophobic barrier drawn around the sections using ImmEdge hydrophobic barrier pen (ACD Bio #310018). Proteins were digested using protease solution (Protease IV) for 30 min at RT. Immediately afterward, slides were washed twice in 0.1 M PBS. C2 and C3 probes were heated in a 40 °C water bath for 10 min, and brought to RT for an additional 10 min. Probes were applied to the slides in a humidified incubator (ACD Bio #321711) for 2 h. Slides were rinsed twice in RNAscope wash buffer and then underwent the colorimetric reaction steps according to the manufacturer's instructions using AMP4-Alt C (C2, far red; C3, green). After the final wash buffer, slides were immediately coverslipped using Prolong Gold Antifade mounting medium with DAPI.

Image analysis

Imaging data for the whole coronal brain section were acquired using an Olympus slide scanner (VS120) for qualitative visualization of transgene expression and viral gene targeting, and analysed in ImageJ using the BIOP VSI reader plugin. Imaging data from immunohistochemistry and smFISH experiments were acquired using an SP8 confocal microscope (Leica) with 20× objective lens (with 1× or 2× zoom) and *z*-stacks (approximately six optical sections with 0.563-µm step size) for three coronal sections per mouse from AP −1.22 mm to −1.70 mm ($n = 3$ mice) were collected. Imaging data were analysed with ImageJ using the Bio-Formats importer plugin. A maximum projection of the *z*-stacks was generated, followed by manual outlining of individual cells and mean fluorescence intensity measurements using the drawing and measure tools. Mean fluorescence intensity values for all cell measurements were normalized to the mean fluorescence intensity for controls.

Statistics

Statistical analyses were performed using GraphPad Prism 8 (GraphPad software) for all data sets. Data are expressed as mean ± s.e.m. Data from two groups were compared using two-tailed unpaired Student's *t*-test. Multiple group comparisons were conducted using one-way ANOVA, or two-way ANOVA, with post hoc tests as described in the Figure legends. Statistical analysis was performed with an α level of 0.05. P values < 0.05 were considered significant.

Reporting summary

Further information on research design is available in the Nature Research Reporting Summary linked to this paper.

Data availability

Details of the statistical analyses are provided in Supplementary Tables 1, 2. The raw behaviour data used in this study are available from the corresponding authors upon request.

Acknowledgements We thank A. Nnenna Chime and S. Taveras for technical assistance; D. Anderson for PKCδ::GluClα-iCre BAC transgenic mice; H. Zeng for the pAAV.CAG Pr.DIO.tTA plasmid; and N. Heintz, A. Nectow and E. Schmidt for the pAAV.Eef1a1 Pr.DIO.eGFP-L10a plasmid. We are grateful to all members of the Klann laboratory for feedback and discussions; and J. Ledoux and R. Del Triano for feedback on this manuscript. This study was supported by National Institute of Health grants NS034007 and NS047384 to E.K., Canadian Institute of Health Research FDN-148366 to J.P., NARSAD Young Investigator grant 26696 to P.S. and a BP-ENDURE fellowship to K.S.A.R. N.H. is supported by a Howard Hughes Medical Investigator grant.

Author contributions P.S. and E.K. conceptualized the framework of this study. P.S. carried out surgeries and behavioural testing, and collected and analysed data. Z.S. carried out western blots and behaviour testing. M.M. performed mouse breeding and pharmacological treatments. K.S.A.R., A.T.Z., C.-Y.J. and P.M.H.-V. carried out mouse behavioural testing. J.P. generated and provided the floxed *Col1a1*$^{\text{TRE GFP.shmiR-4E}}$ mice. N.H. generated and provided the floxed iPKR mice. P.S. and E.K. wrote the paper. All authors read and commented on the paper.

Competing interests The authors declare no competing financial interests.

Additional information
Supplementary information is available for this paper at https://doi.org/10.1038/s41586-020-2793-8.
Correspondence and requests for materials should be addressed to P.S. or E.K.
Peer review information *Nature* thanks Richard Palmiter and the other, anonymous, reviewer(s) for their contribution to the peer review of this work.
Reprints and permissions information is available at http://www.nature.com/reprints.

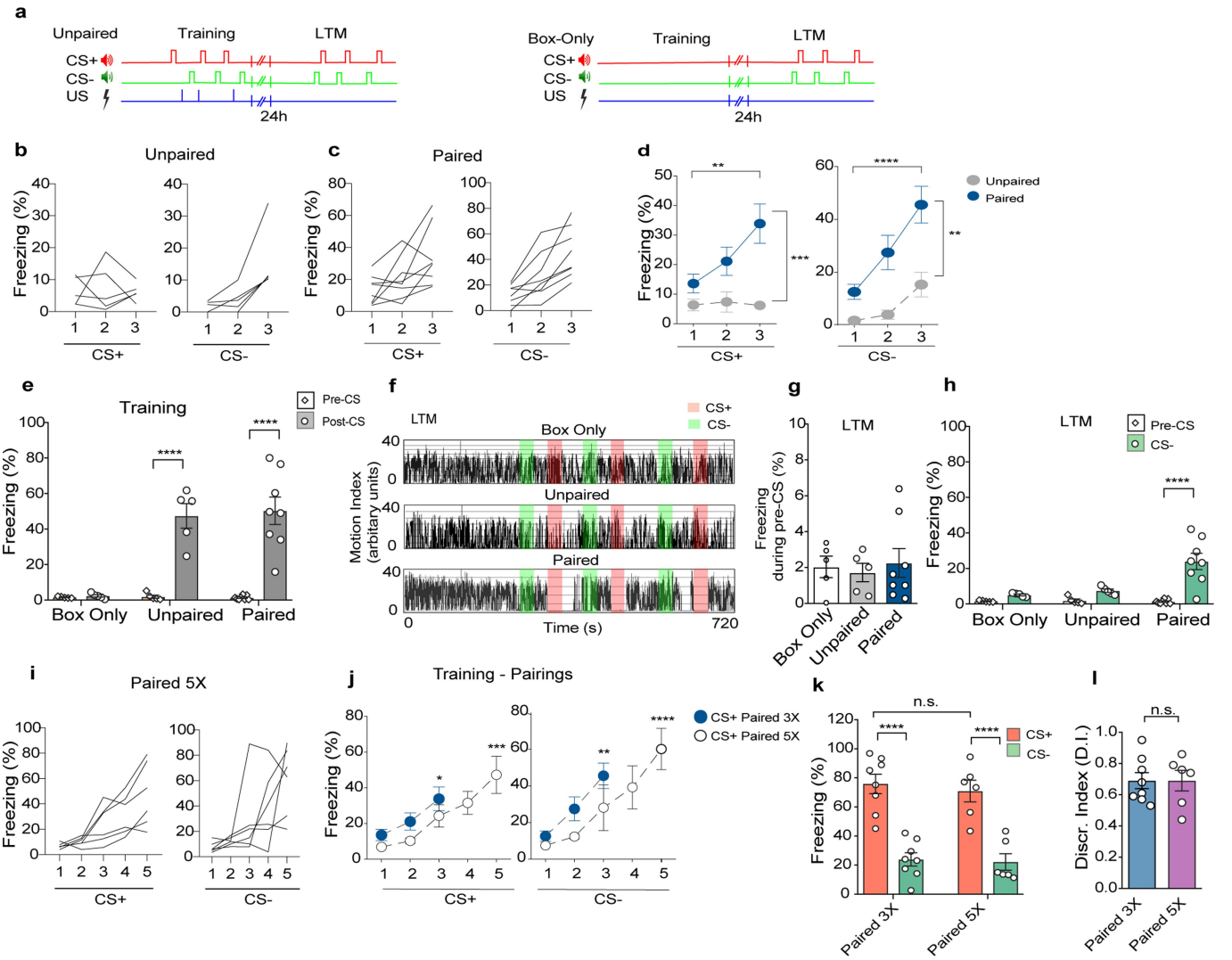

Extended Data Fig. 1 | Differential cued threat conditioning. a, Schematic of the behaviour protocol for the Unpaired group (left) and Box-Only control group (right). **b**, Freezing response to CS+ and CS- in individual animals trained using the Unpaired behaviour protocol. **c**, Freezing response to CS+ and CS- in individual animals trained using the Paired behaviour protocol. **d**, Paired group learned the association between CS+ and US and showed increasing freezing response to successive CS presentations whereas the Unpaired group did not associate CS+ with US. RM Two-way ANOVA with Bonferroni's post hoc test. Effect of CS+ training: $F(1,11) = 11.40$, $P = 0.0062$; effect of CS- training: $F(2,33) = 9.360$, $P = 0.0006$. n[Unpaired] = 5 and n[Paired] = 8 animals. **e**, Both Paired and Unpaired groups, but not Box-Only group, increased freezing levels during the post-tone period compared to the pre-tone period. Two way ANOVA with Bonferroni's post hoc test. Effect of training: $F(2,30) = 13.86$, $P < 0.0001$, effect of epoch: $F(1,30) = 60.38$, $P < 0.0001$. n[Box-Only] = 5, n[Unpaired] = 5 and n[Paired] = 8 animals. **f**, Representative motion traces for Box-Only, Unpaired and Paired groups during LTM. **g**, Freezing response during pre-CS of LTM test is low for all three groups. One-way ANOVA. $P = 0.874$. n[Box-Only] = 5, n[Unpaired] = 5 and n[Paired] = 8 animals. **h**, Animals in the Paired group freeze significantly higher during CS- than during the pre-tone period. Two-way ANOVA with Bonferroni's post hoc test. Effect of training: $F(2,30) = 8.38$, $P = 0.0013$; effect of epoch: $F(1,30) = 23.97$, $P < 0.0001$. n[Box-Only] = 5, n[Unpaired] = 5 and n[Paired] = 8 animals. **i**, Freezing response to CS+ and CS- in individual animals trained using the Paired 5X behaviour protocol. **j**, Increasing the number of CS-US pairs from 3 to 5 pairings during training led to a continued escalation of freezing response to successive presentations of CS's. RM Two-way ANOVA with Bonferroni's post hoc test. Effect of CS+: $F(1,24) = 23.95$, $P < 0.0001$; effect of CS-: $F(1,24) = 42.74$, $P < 0.0001$. Paired 3X CS+: CS1 vs CSn, $P = 0.039$; Paired 5X CS+: CS1 vs CSn, $P = 0.0005$. n[Paired 3X] = 8 and n[Paired 5X] = 6 animals. **k**, Paired 5X group displayed equivalent conditioned threat response and safety response to CS+ and CS- respectively as paired 3X group during LTM test. Two way ANOVA with Bonferroni's post hoc test. Effect of pairings: $F(1,24) = 0.2942$, $P = 0.593$; effect of CS: $F(1,24) = 66.46$, $P < 0.0001$. n[Paired 3X] = 8 and n[Paired 5X] = 6 animals. **l**, Discrimination index for cued threat in Paired 5X group was unaltered compared to Paired 3X group. Unpaired *t*-test, Two-tailed. $P > 0.999$. Data are presented as mean ± s.e.m. $^{*}P < 0.05$, $^{**}P < 0.01$, $^{***}P < 0.001$, $^{****}P < 0.0001$. n.s. nonsignificant.

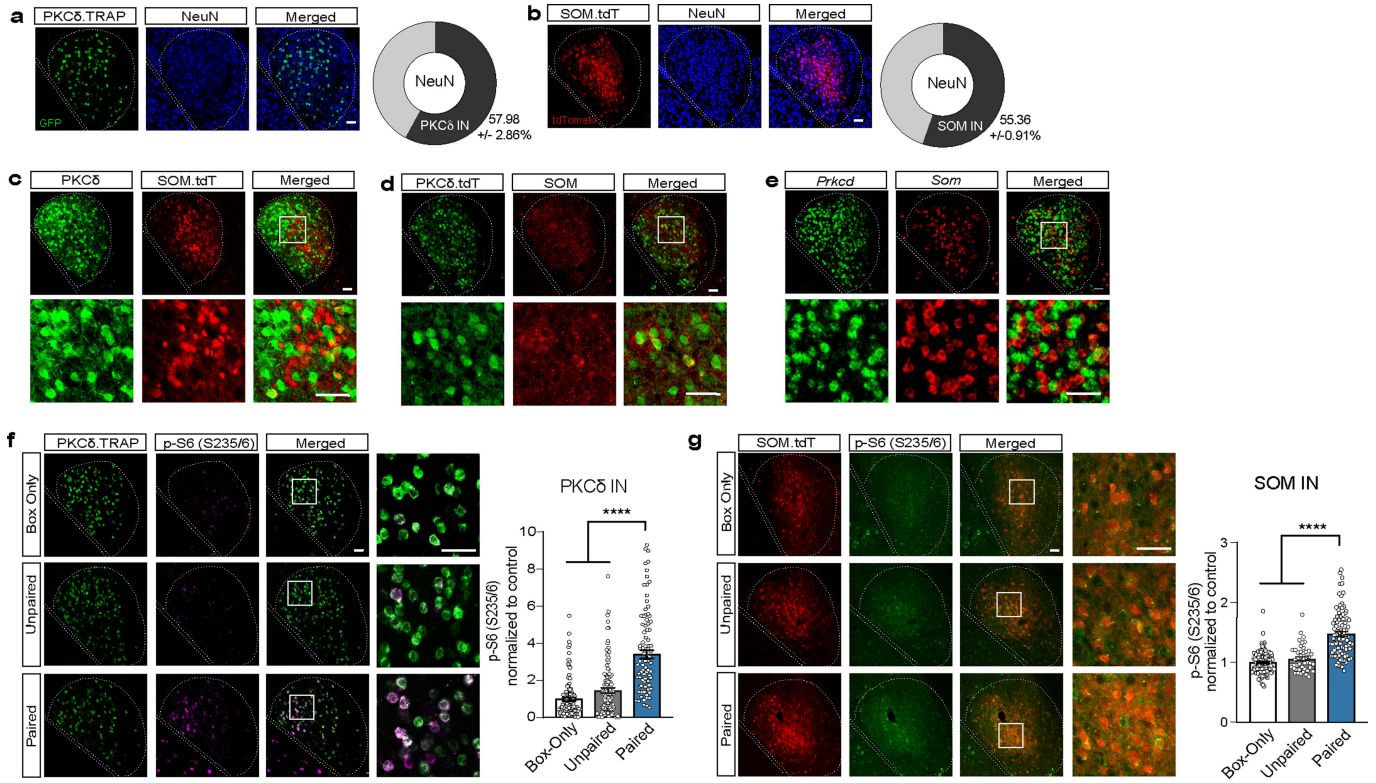

Extended Data Fig. 2 | Distinct IN subpopulations in centrolateral amygdala. **a**, Co-immunostaining for GFP and neuronal marker, NeuN, in PKCδ.TRAP amygdala sections. 57.96 ± 2.86% of all neurons in centrolateral amygdala are PKCδ INs. *n* = 3 animals/group. **b**, Co-immunostaining for tdTomato and NeuN in SOM.tdT amygdala sections. SOM INs constitute 55.36 ± 0.91% of all neurons in CeL. *n* = 3 animals/group. **c**, Immunohistochemistry for PKCδ in SOM.tdT brain sections shows largely non-overlapping expression of PKCδ in SOM Cre expressing cells in CeL. **d**, Immunohistochemistry for SOM in PKCδ.tdT brain sections also shows largely non-overlapping populations but the subcellular distribution of SOM in neuronal processes makes it difficult to analyse the extent of SOM co-expression in PKCδ Cre expressing cell populations. **e**, Multiplexed smFISH for *Prkcd* and *Som* showing mutually exclusive INs in CeL expressing these two mRNA populations. **f**, Immunohistochemistry data for PKCδ.TRAP amygdala sections showing expression of p-S6 (S235/6) in PKCδ neurons in CeL across three groups (Box-Only, Unpaired and Paired) at 30 min post training. One-way ANOVA with Bonferroni's post hoc test. $F(2,334) = 71.67$, $P < 0.0001$. n[Box-Only] = 117, n[Unpaired] = 118 and n[Paired] = 102 cells from 3 animals/group. **g**, Immunohistochemistry data for SOM tdTomato sections showing p-S6 (S235/6) in SOM neurons in CeL across groups. One-way ANOVA with Bonferroni's post hoc test. $F(2,292) = 44.18$, $P < 0.0001$. n[Box-Only] = 162, n[Unpaired] = 158 and n[Paired] = 165 cells from 3 animals/group. Scale bar, 50 µm.

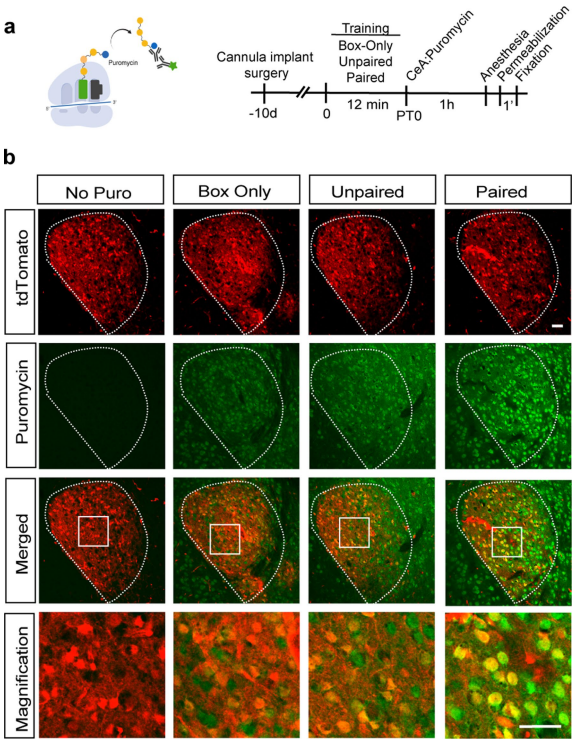

Extended Data Fig. 3 | Differential threat conditioning induces de novo translation in CeL neurons. a, Schematic for the in vivo de novo translation labelling assay with puromycin infusion in central amygdala. **b**, De novo translation was upregulated in PKCδ INs in the Paired training group compared to Box-Only and Unpaired controls. Insets show higher magnification.

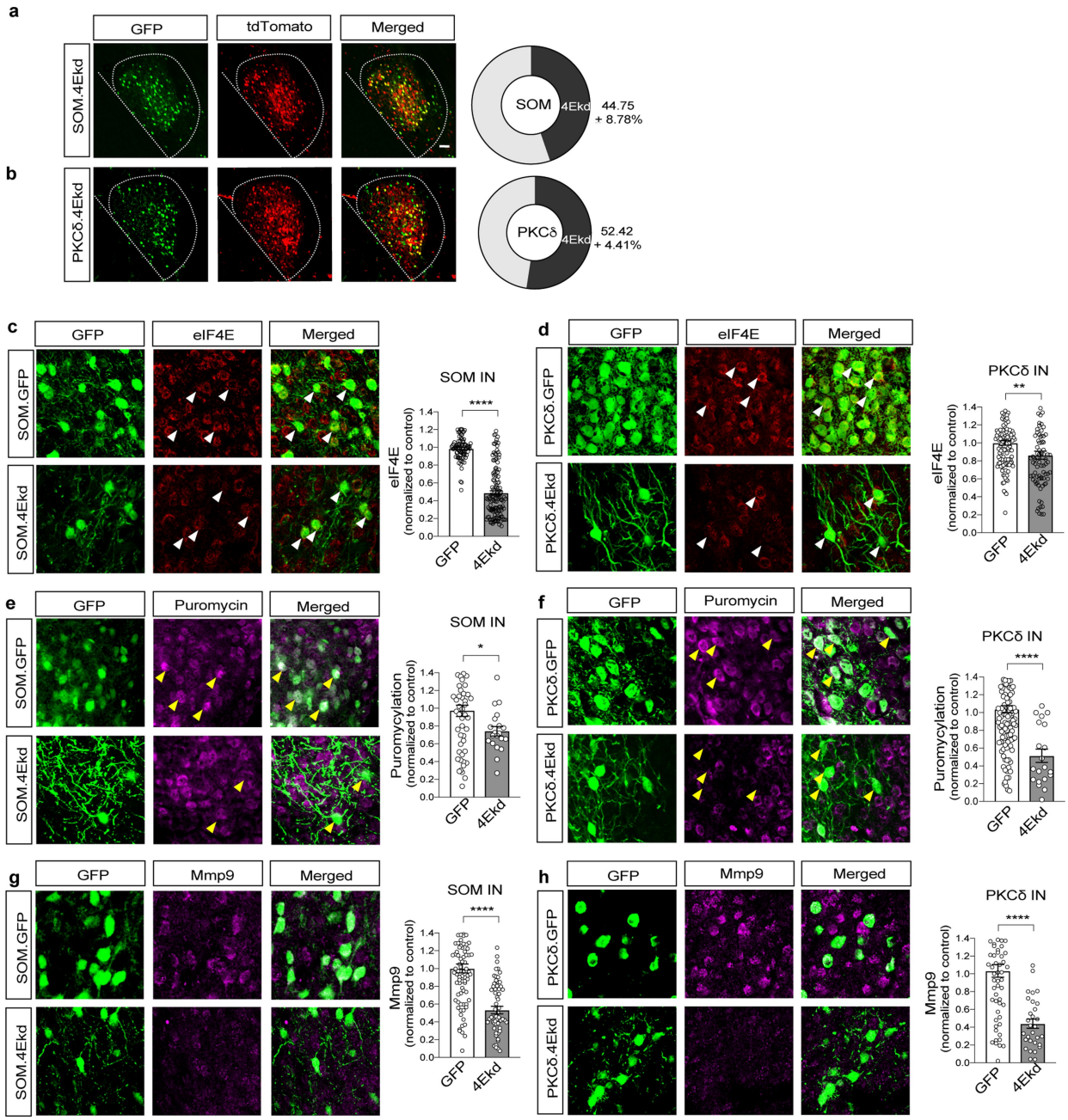

Extended Data Fig. 4 | Cell-type-specific knockdown of cap dependent translation in CeL neurons. a, Proportion of endogenous SOM.tdT INs chemogenetically targeted to express shmir-eIF4E in a cre- and tet-dependent manner. 44.75 ± 8.78% of SOM.tdT INs in CeL expressed shmir-eIF4E. $n = 3$ animals/group. **b**, Proportion of endogenous PKCδ.tdT INs chemogenetically targeted to express shmir-eIF4E in a cre- and tet-dependent manner. 52.42+4.41% of PKCδ.tdT INs in CeL expressed shmir-eIF4E. $n = 3$ animals/group. **c**, eIF4E level was significantly reduced in SOM INs in SOM.4Ekd group compared to SOM.GFP control. Unpaired *t*-test, Two-tailed. $P < 0.0001$. n[SOM.GFP] = 87 and n[SOM.4Ekd] = 132 cells from 3 animals/group. **d**, eIF4E level was significantly knocked down in PKCδ INs in PKCδ.4Ekd group compared to PKCδ.GFP control. Unpaired *t*-test, Two-tailed. $P = 0.0056$, n[PKCδ.GFP] = 121 and n[PKCδ.4Ekd] = 87 cells from 3 animals/group. **e**, Global de novo translation, as measured with puromycin assay, was significantly reduced in SOM.4Ekd group compared to control. Unpaired *t*-test, Two-tailed. $P = 0.0363$. n[SOM.GFP] = 53 and n[SOM.4Ekd] = 20 cells from 3 animals/ group. **f**, Similarly, global de novo protein synthesis was significantly diminished in PKCδ.4Ekd group compared to control. Unpaired *t*-test, Two-tailed. $P < 0.0001$. n[PKCδ.GFP] = 120 and n[PKCδ.4Ekd] = 20 cells from 4 animals/ group. **g**, MMP9 levels was significantly reduced in SOM.4Ekd mice compared to control. Unpaired *t*-test, Two-tailed. $P < 0.0001$. n[SOM.GFP] = 87 and n[SOM.4Ekd] = 60 cells from 3 animals/group. **h**, Similarly, MMP9 level was significantly reduced in PKCδ.4Ekd group compared to control. Unpaired *t*-test, Two-tailed. $P < 0.0001$. n[PKCδ.GFP] = 60 and n[PKCδ.4Ekd] = 30 cells from 3 animals/group. Data are presented as mean + s.e.m. $^*P < 0.05$, $^{**}P < 0.01$, $^{***}P < 0.001$, $^{****}P < 0.0001$. n.s. nonsignificant. Scale bar, 50 µm.

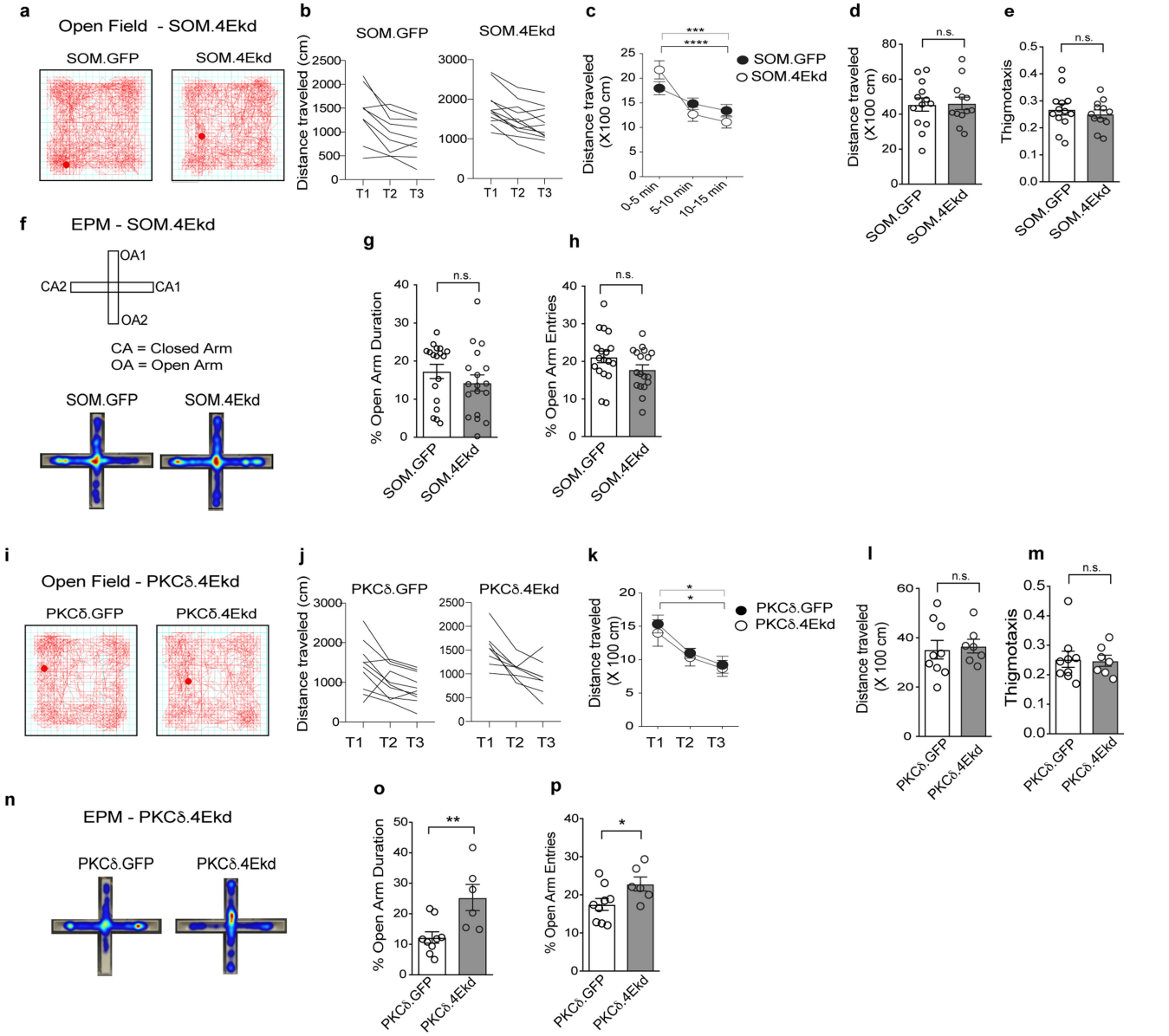

Extended Data Fig. 5 | Inhibition of cap-dependent translation and anxiety related behaviours. a, Representative open field activity traces for SOM.GFP and SOM.4Ekd animals. **b**, Distance travelled in the open field arena for individual SOM.GFP and SOM.4Ekd animals. **c**, XY plot showing normal acclimation of SOM.GFP and SOM.4Ekd animals to the open field arena. Effect of Time: $F(2,46) = 45.50$, $P < 0.0001$. n[SOM.GFP] = 13 and n[SOM.4Ekd] = 12 animals. **d**, SOM.GFP and SOM.4Ekd animals display equivalent spontaneous locomotion in the open field arena. Unpaired *t*-test, Two-tailed. $P = 0.895$. n[SOM.GFP] = 13 and n[SOM.4Ekd] = 12 animals. **e**, SOM.4Ekd mice display normal thigmotaxis behaviour compared to control. Unpaired *t*-test, Two-tailed. $P = 0.521$. n[SOM.GFP] = 13 and n[SOM.4Ekd] = 12 animals. **f**, Representative activity heat map in elevated plus maze for SOM.GFP and SOM.4Ekd animals. **g**, SOM.GFP and SOM.4Ekd animals spend similar duration in the open arm, as a percent of total duration. Unpaired *t*-test, Two-tailed. $P = 0.288$. n[SOM.GFP] = 18 and n[SOM.4Ekd] = 18 animals. **h**, SOM.GFP and SOM.4Ekd mice make equivalent entries into the open arm. Unpaired *t*-test, Two-tailed. $P = 0.107$. n[SOM.GFP] = 18 and n[SOM.4Ekd] = 18 animals. **i**, Representative open field activity traces for PKCδ.GFP and PKCδ.4Ekd animals. **j**, Distance travelled in the open field arena for individual PKCδ.GFP and PKCδ.4Ekd animals. **k**, XY plot showing normal acclimation of PKCδ.GFP and PKCδ.4Ekd animals to the open field arena. RM Two-way ANOVA. Time: $F(2,32) = 19.12$, $P < 0.0001$. n[PKCδ.GFP] = 10 and n[PKCδ.4Ekd] = 8 animals. **l**, Bar plot showing total distance travelled by PKCδ WT and PKCδ 4Ekd mice in the open field arena. Unpaired *t*-test, Two-tailed. $P = 0.772$. n[PKCδ.GFP] = 10 and n[PKCδ.4Ekd] = 8 animals. **m**, PKCδ.4Ekd mice show normal thigmotaxis in the open field arena compared to PKCδ.GFP control. Unpaired *t*-test, Two-tailed. $P = 0.888$. n[PKCδ.GFP] = 7 and n[PKCδ.4Ekd] = 9 animals. **n**, Representative activity heat maps in elevated plus maze for PKCδ.GFP and PKCδ.4Ekd animals. **o**, Bar plot showing significantly increased %time spent in the open arm for PKCδ.4Ekd animals compared to PKCδ.GFP controls. Unpaired *t*-test, Two-tailed. $P = 0.0074$. n[PKCδ.GFP] = 9 and n[PKCδ.4Ekd] = 6 animals. **p**, Bar plot showing % entries into the open arm for PKCδ.4Ekd animals compared to PKCδ.GFP controls. $P = 0.0476$. n[PKCδ.GFP] = 9 and n[PKCδ.4Ekd] = 6 animals. Data are presented as mean + s.e.m. $^{**}P < 0.01$, $^{****}P < 0.0001$, n.s. nonsignificant.

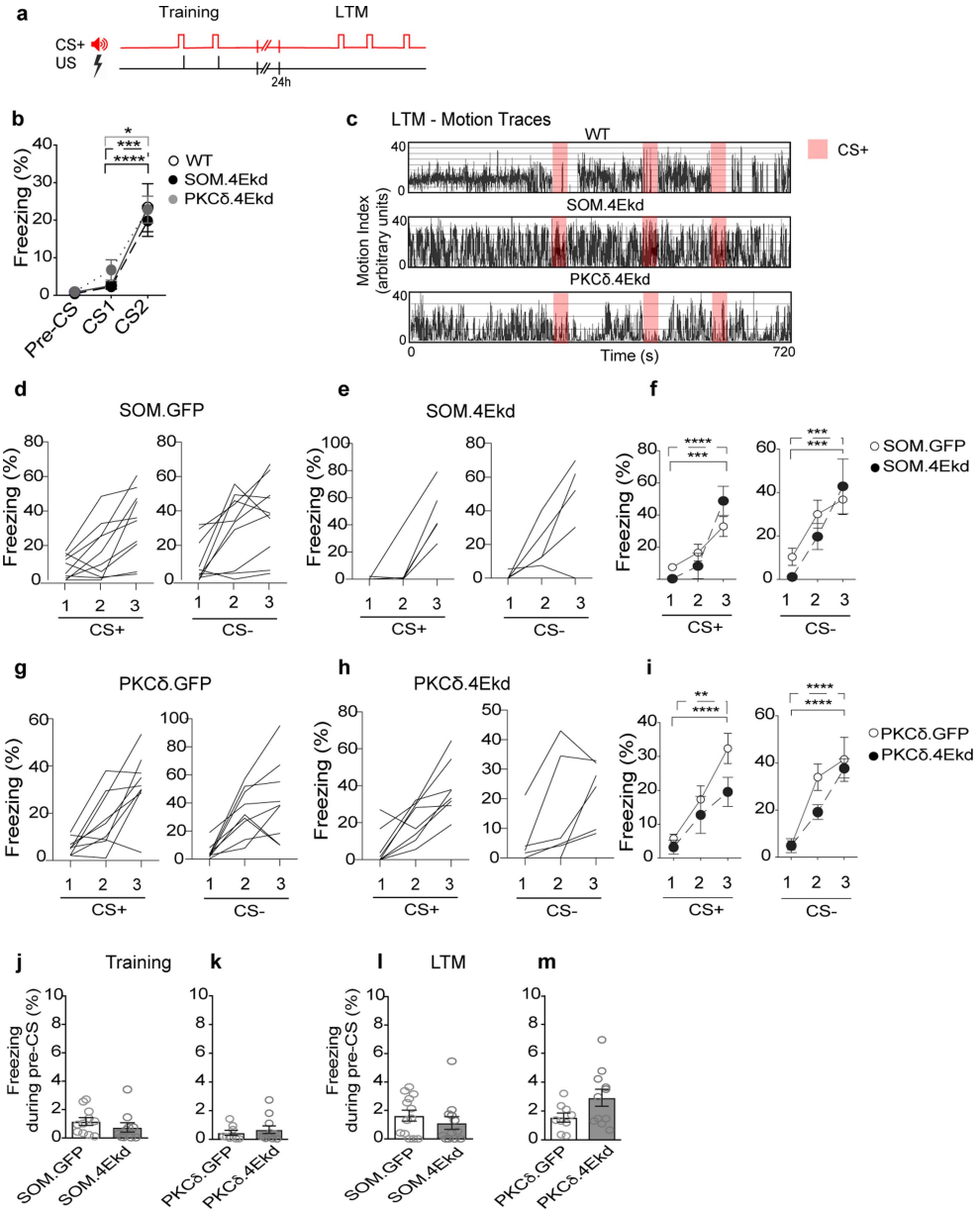

Extended Data Fig. 6 | Inhibition of cap-dependent translation in CeL INs and simple threat conditioning. a, Schematic for simple threat conditioning paradigm in SOM and PKCδ 4Ekd mice. **b**, Normal memory acquisition in simple threat-conditioning in WT, SOM.4Ekd and PKCδ 4Ekd groups. Effect of CS: $F(2,50) = 32.28$, $P < 0.0001$. n[WT] = 12, n[SOM.4Ekd] = 11 and n[PKCδ.4Ekd] = 5 animals. **c**, Representative motion traces for WT, SOM.4Ekd and PKCδ.4Ekd groups during LTM test. **d**, Freezing response to CS+ and CS- in individual SOM.GFP animals during training. **e**, Freezing response to CS+ and CS- in individual SOM.4Ekd animals during training. **f**, Normal memory acquisition in differential threat conditioning in SOM.GFP and SOM.4Ekd mice. Effect of CS+: $F(2,26) = 34.66$, $P < 0.0001$; effect of CS-: $F(2,26) = 20.81$, $P < 0.0001$. n[SOM.GFP] = 10 and n[SOM.4Ekd] = 5 animals. **g**, Freezing response to CS+ and CS- in individual PKCδ.GFP animals during training. **h**, Freezing response to CS+ and CS- in individual PKCδ.4Ekd animals during training. **i**, Normal memory acquisition in PKCδ.GFP and PKCδ.4Ekd mice. Effect of CS+: $F(2,34) = 24.67$, $P < 0.0001$; effect of CS-: $F(2,34) = 36.84$, $P < 0.0001$. n[PKCδ.GFP] = 9 and n[PKCδ.4Ekd] = 10 animals. **j**, SOM.4Ekd mice have negligible freezing response during pre-CS in Training phase compared to controls. Unpaired *t*-test, Two-tailed. $P = 0.341$. n[SOM.GFP] = 11 and n[SOM.4Ekd] = 10 animals. **k**, PKCδ.4Ekd mice have negligible freezing response during pre-CS in the Training phase compared to controls. Unpaired *t*-test, Two-tailed. $P = 0.541$. n[PKCδ.GFP] = 8 and n[PKCδ.4Ekd] = 11 animals. **l**, SOM.4Ekd mice have comparable low freezing response during pre-CS in LTM test compared to controls. Unpaired *t*-test, Two-tailed. $P = 0.389$. n[SOM.GFP] = 13 and n[SOM.4Ekd] = 12 animals. **m**, PKCδ.4Ekd mice have comparable low freezing response during pre-CS in LTM test compared to controls. Unpaired *t*-test, Two-tailed. $P = 0.068$. n[PKCδ.GFP] = 9 and n[PKCδ.4Ekd] = 11 animals. Data are presented as mean + s.e.m. $^{**}P < 0.01$, $^{****}P < 0.0001$, n.s. nonsignificant.

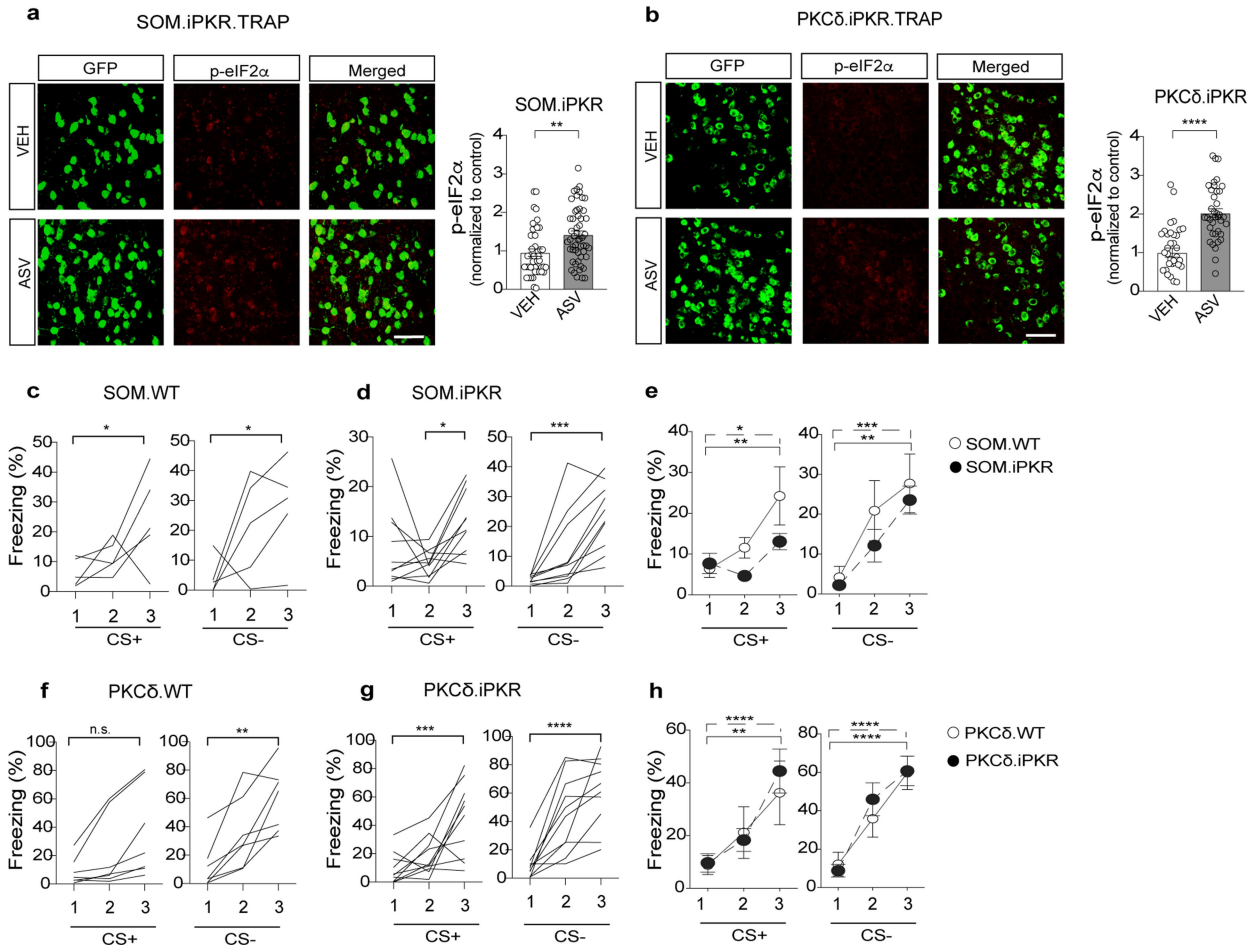

Extended Data Fig. 7 | Cell type-specific eIF2α phosphorylation and threat conditioning. a, Compared to vehicle controls, ASV infusion in the central amygdala of SOM.iPKR.TRAP animals significantly increased phosphorylation of eIF2α in SOM neurons. Unpaired *t*-test, Two-tailed. $P = 0.0013$. n[SOM.iPKR.TRAP +VEH] = 43 and n[SOM.iPKR.TRAP +ASV] = 53 cells from 3 animals/ group. **b**, ASV infusion in CeA of PKCδ.iPKR.TRAP mice also significantly elevated p-eIF2α in PKCδ neurons compared to vehicle control. Unpaired *t*-test, Two-tailed. $P < 0.0001$. n[PKCδ.iPKR.TRAP +VEH] = 36 and n[PKCδ.iPKR.TRAP +ASV] = 38 cells from 3 animals/ group. **c**, Freezing response to CS+ and CS- in individual SOM.WT animals during training. **d**, Freezing response to CS+ and CS- in individual SOM.iPKR animals during training. **e**, Normal memory acquisition in SOM.WT and SOM.iPKR animals in differential threat conditioning paradigm. RM Two-way ANOVA with Bonferroni's post hoc test. Effect of CS+: $F(2,26) = 10.98$, $P = 0.0003$; effect of CS-: $F(2,26) = 18.40$, $P < 0.0001$. n[SOM.WT] = 5 and n[SOM.iPKR] = 10 animals. **f**, Freezing response to CS+ and CS- in individual PKCδ.WT animals during training. **g**, Freezing response to CS+ and CS- in individual PKCδ.iPKR animals during training. **h**, Normal memory acquisition in PKC.WT and PKC.iPKR animals in differential threat conditioning paradigm. RM Two-way ANOVA with Bonferroni's post hoc test. Effect of CS+: $F(2,30) = 18.70$, $P < 0.0001$; effect of CS-: $F(2,30) = 46.39$, $P < 0.0001$. n[PKC.WT] = 7 and n[PKC.iPKR] = 10 animals. Data are presented as mean + s.e.m. $^{**}P < 0.01$, $^{****}P < 0.0001$. Scale bar, 50 µm.

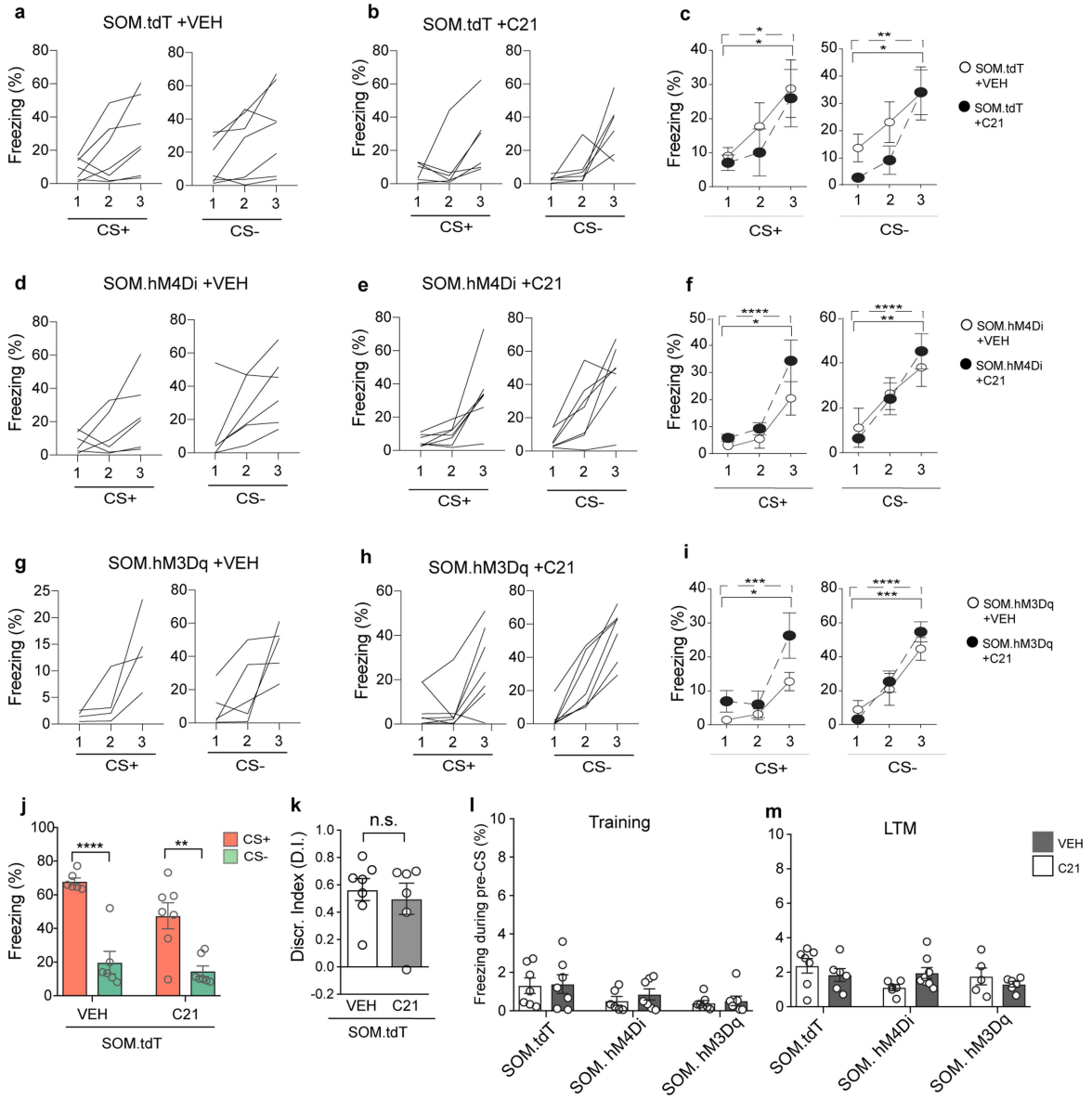

Extended Data Fig. 8 | Chemogenetic modulation of G-protein signalling in CeL SOM INs affects associative learning. a, Freezing response to CS+ and CS- in individual SOM.tdT animals treated with vehicle during training. **b**, Freezing response to CS+ and CS- in individual SOM.tdT animals treated with C21 during training. **c**, C21 treated SOM.tdT mice learn normally compared to VEH treated controls. RM Two-way ANOVA with Bonferroni's post hoc test. Effect of CS+: $F(2,22) = 8.02$, $P = 0.0024$; effect of CS-: $F(2,22) = 17.00$, $P < 0.0001$. n[SOM.tdT +VEH] = 7 and n[SOM.tdT +C21] = 6 animals. **d**, Freezing response to CS+ and CS- in individual SOM.hM4Di animals treated with vehicle during training. **e**, Freezing response to CS+ and CS- in individual SOM.hM4Di animals treated with C21 during training. **f**, C21 treated SOM.hM4Di mice have normal memory acquisition relative to VEH controls. RM Two-way ANOVA with Bonferroni's post hoc test. CS+: $F(2,22) = 20.62$, $P < 0.0001$; CS-: $F(2,22) = 19.62$, $P < 0.0001$. n[SOM.hM4Di +VEH] = 6 and n[SOM.hM4Di +C21] = 7 animals. **g**, Freezing response to CS+ and CS- in individual SOM.hM3Dq animals treated with vehicle during training. **h**, Freezing response to CS+ and CS- in individual SOM.hM3Dq animals treated with C21 during training. **i**, C21 treated SOM.hM3Dq animals acquire differential threat memory normally relative to VEH controls. RM Two-way ANOVA with Bonferroni's post hoc test. Effect of CS+: $F(2,20) = 17.09$, $P < 0.0001$; effect of CS-: $F(2,20) = 38.94$, $P < 0.0001$. n[SOM.hM4Di +VEH] = 5 and n[SOM.hM4Di +C21] = 7 animals. **j**, C21 treated SOM.tdT mice exhibit normal threat and safety LTM response to CS+ and CS- respectively. RM Two-way ANOVA with Bonferroni's post hoc test. Effect of drug: $F(1,22) = 5.233$, $P = 0.0321$; effect of CS: $F(1,22) = 52.87$, $P < 0.0001$. n[SOM.tdT +VEH] = 7 and n[SOM.tdT +C21] = 6 animals. **k**, C21 treatment does not alter cued threat discrimination index in SOM.tdT mice. Unpaired *t*-test, Two-tailed. $P = 0.6313$. n[SOM.tdT +VEH] = 7 and n[SOM.tdT +C21] = 6 animals. **l**, Freezing response during pre-CS of training session is negligible across all C21 and VEH treated SOM groups. Two-way ANOVA. Effect of drug: $F(2,31) = 2.410$, $P = 0.1064$. n[SOM.tdT +VEH] = 7, n[SOM.tdT +C21] = 6, n[SOM.hM4Di +VEH] = 6, n[SOM.hM4Di +C21] = 7, n[SOM.hM3Dq +VEH] = 4 and n[SOM.hM3Dq +C21] = 7 animals. **m**, C21 treated SOM.tdT, SOM.hM4Di and SOM.hM3Dq mice have equivalent freezing response during pre-CS of LTM test compared to VEH controls. Two-way ANOVA. Effect of drug: $F(2.32) = 1.899$, $P = 0.1663$. n[SOM.tdT +VEH] = 7, n[SOM.tdT +C21] = 6, n[SOM.hM4Di +VEH] = 6, n[SOM.hM4Di +C21] = 8, n[SOM.hM3Dq +VEH] = 5 and n[SOM.hM3Dq +C21] = 6 animals. Data are presented as mean ± s.e.m. $^*P < 0.05$, $^{**}P < 0.01$, $^{***}P < 0.001$, $^{****}P < 0.0001$. n.s. nonsignificant.

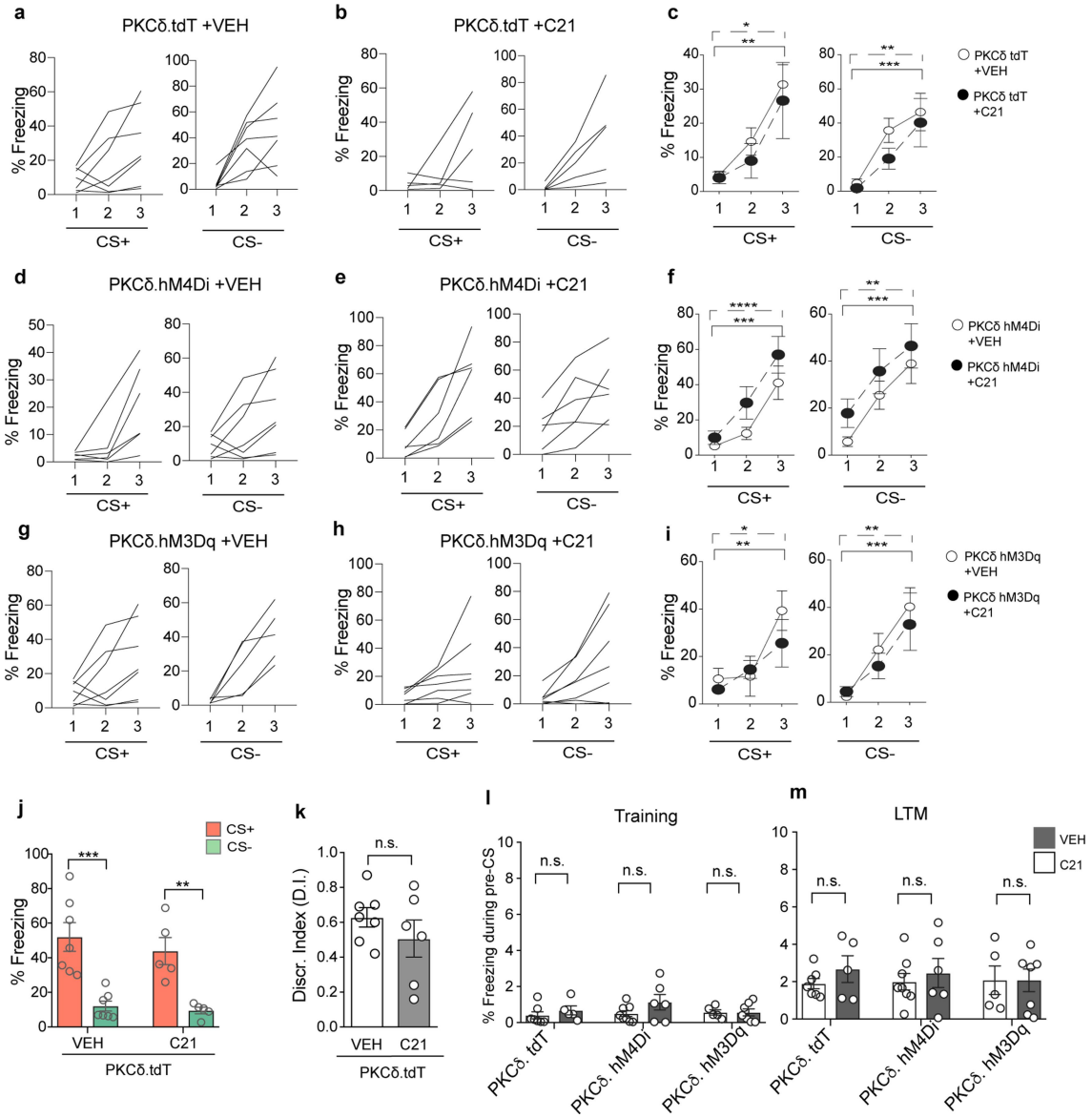

Extended Data Fig. 9 | Chemogenetic modulation of G-protein signalling in CeL PKCδ INs affects associative learning. a, Freezing response to CS+ and CS- in individual PKCδ.tdT animals treated with vehicle during training. **b**, Freezing response to CS+ and CS- in individual PKCδ.tdT animals treated with C21 during training. **c**, C21 treated PKCδ.tdT animals have normal memory acquisition relative to VEH controls, with progressive increase in freezing response to successive presentation of CS's. RM Two-way ANOVA with Bonferroni's post hoc test. Effect of CS+: $F(2,20) = 12.22$, $P = 0.0003$; effect of CS-: $F(2,20) = 18.65$, $P < 0.0001$. n[PKCδ.tdT +VEH] = 7 and n[PKCδ.tdT +C21] = 5 animals. **d**, Freezing response to CS+ and CS- in individual PKCδ.hM4Di animals treated with vehicle during training. **e**, Freezing response to CS+ and CS- in individual PKCδ.hM4Di animals treated with C21 during training. **f**, C21 treated PKCδ.hM4Di animals learn normally compared to VEH controls. RM Two-way ANOVA with Bonferroni's post hoc test. Effect of CS+: $F(2,24) = 29.92$, $P < 0.0001$; effect of CS-: $F(2,24) = 19.58$, $P < 0.0001$. n[PKCδ.hM4Di +VEH] = 8 and n[PKCδ.hM4Di +C21] = 6 animals. **g**, Freezing response to CS+ and CS- in individual PKCδ.hM3Dq animals treated with vehicle during training. **h**, Freezing response to CS+ and CS- in individual PKCδ.hM3Dq animals treated with C21 during training. **I**, C21 treated PKCδ.hM3Dq animals acquire differential threat memory normally compared to VEH controls. RM Two-way ANOVA with Bonferroni's post hoc test. Effect of CS+: $F(2,20) = 15.90$, $P < 0.0001$; effect of CS-: $F(2,20) = 20.67$, $P < 0.0001$. n[PKCδ.hM3Dq +VEH] = 5 and n[PKCδ.hM3Dq +C21] = 7 animals. **j**, C21 treated PKCδ.tdT mice exhibit normal threat and safety LTM response to CS+ and CS- respectively. RM Two-way ANOVA with Bonferroni's post hoc test. Effect of CS: $F(1,20) = 0.402$. n[PKCδ.tdT +VEH] = 7 and n[PKCδ.tdT +C21] = 5 animals. **k**, C21 treatment does not alter cued threat discrimination index in PKCδ.tdT mice. Unpaired *t*-test, Two-tailed. $P = 0.3116$. n[PKCδ.tdT +VEH] = 7 and n[PKCδ.tdT +C21] = 6 animals. **l**, Freezing response during pre-CS of the training session is negligible across all C21 and VEH treated PKCδ groups. Two-way ANOVA. Effect of drug: $F(2,35) = 0.2326$, $P = 0.794$. n[PKCδ.tdT +VEH] = 7, n[PKCδ.tdT +C21] = 6, n[PKCδ.hM4Di +VEH] = 8, [PKCδ.hM4Di +C21] = 6, n[PKCδ.hM3Dq +VEH] = 5 and n[PKCδ.hM3Dq +C21] = 7 animals. **m**, C21 treatment in PKCδ.tdT, PKCδ. hM4Di and PKCδ.hM3Dq animals does not alter baseline freezing response during pre-CS of LTM test. Two-way ANOVA. Effect of drug: $F(2,32) = 0.0171$, $P = 0.983$. n[PKCδ.tdT +VEH] = 7, n[PKCδ.tdT +C21] = 5, n[PKCδ.hM4Di +VEH] = 8, [PKCδ.hM4Di +C21] = 6, n[PKCδ.hM3Dq +VEH] = 5 and n[PKCδ. hM3Dq +C21] = 7 animals. Data are presented as mean ± s.e.m. $^{*}P < 0.05$, $^{**}P < 0.01$, $^{***}P < 0.001$, $^{****}P < 0.0001$. n.s. nonsignificant.

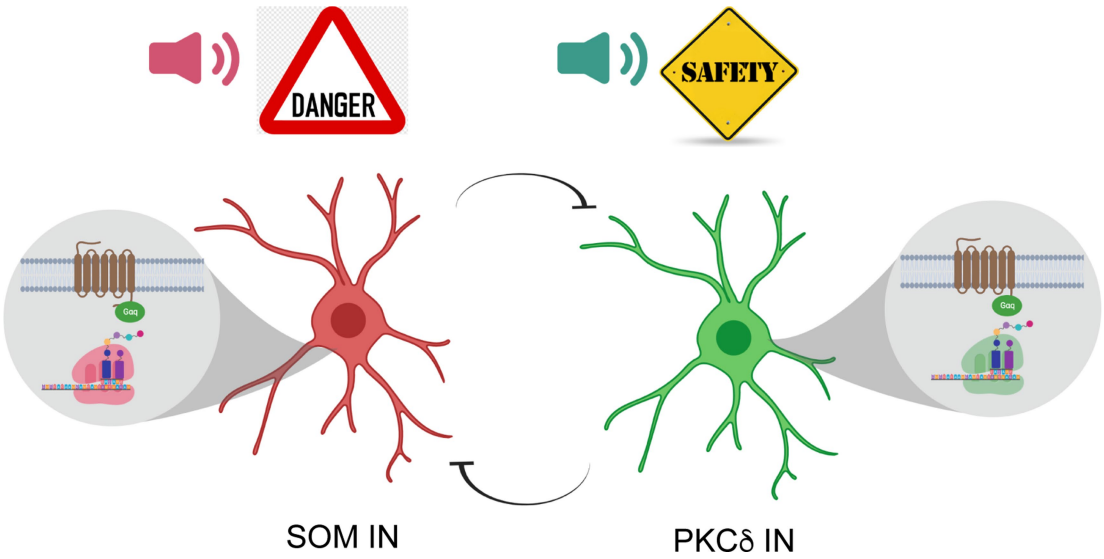

Extended Data Fig. 10 | Working model of simultaneous consolidation and storage of threat and safety cue-associated memories in CeL SOM and PKCδ INs, respectively. In a differential threat conditioning paradigm, cued threat mobilizes the translation machinery in CeL SOM INs via activation of Gq-coupled GPCR(s), and the ensuing de novo protein synthesis in these neurons is necessary for long-term storage of a cued threat response. The cued safety signal, on the other hand, is processed by CeL PKCδ INs with engagement of the cell-autonomous protein synthesis machinery, leading to long-term storage of the cued safety response.

nature research

Corresponding author(s): Eric Klann, Prerana Shrestha

Last updated by author(s): 06-08-2020

Reporting Summary

Nature Research wishes to improve the reproducibility of the work that we publish. This form provides structure for consistency and transparency in reporting. For further information on Nature Research policies, see our Editorial Policies and the Editorial Policy Checklist.

Statistics

For all statistical analyses, confirm that the following items are present in the figure legend, table legend, main text, or Methods section.

n/a	Confirmed	
☐	☒	The exact sample size (*n*) for each experimental group/condition, given as a discrete number and unit of measurement
☐	☒	A statement on whether measurements were taken from distinct samples or whether the same sample was measured repeatedly
☐	☒	The statistical test(s) used AND whether they are one- or two-sided *Only common tests should be described solely by name; describe more complex techniques in the Methods section.*
☐	☒	A description of all covariates tested
☐	☒	A description of any assumptions or corrections, such as tests of normality and adjustment for multiple comparisons
☐	☒	A full description of the statistical parameters including central tendency (e.g. means) or other basic estimates (e.g. regression coefficient) AND variation (e.g. standard deviation) or associated estimates of uncertainty (e.g. confidence intervals)
☐	☒	For null hypothesis testing, the test statistic (e.g. *F*, *t*, *r*) with confidence intervals, effect sizes, degrees of freedom and *P* value noted *Give P values as exact values whenever suitable.*
☒	☐	For Bayesian analysis, information on the choice of priors and Markov chain Monte Carlo settings
☒	☐	For hierarchical and complex designs, identification of the appropriate level for tests and full reporting of outcomes
☒	☐	Estimates of effect sizes (e.g. Cohen's *d*, Pearson's *r*), indicating how they were calculated

Our web collection on statistics for biologists contains articles on many of the points above.

Software and code

Policy information about availability of computer code

Data collection	FreezeFrame3, Noldus Ethovision XT13, Activity monitor (Med Associates), ProteinSimple, Leica imaging software LASX
Data analysis	We used GraphPad Prism 8 to analyze behavior data. We used ImageJ to analyze confocal images and Western Immunoblots.

For manuscripts utilizing custom algorithms or software that are central to the research but not yet described in published literature, software must be made available to editors and reviewers. We strongly encourage code deposition in a community repository (e.g. GitHub). See the Nature Research guidelines for submitting code & software for further information.

Data

Policy information about availability of data

All manuscripts must include a data availability statement. This statement should provide the following information, where applicable:

- Accession codes, unique identifiers, or web links for publicly available datasets
- A list of figures that have associated raw data
- A description of any restrictions on data availability

Provide your data availability statement here.

Field-specific reporting

Please select the one below that is the best fit for your research. If you are not sure, read the appropriate sections before making your selection.

☒ Life sciences ☐ Behavioural & social sciences ☐ Ecological, evolutionary & environmental sciences

For a reference copy of the document with all sections, see nature.com/documents/nr-reporting-summary-flat.pdf

Life sciences study design

All studies must disclose on these points even when the disclosure is negative.

Sample size	Sample size were estimated based on published research from our lab using similar chemogenetic and pharmacological manipulations in mice such as Huynh, H., Santini, E., & Klann, E. J Neurosci 34(27): 9034-9039 (2014). PMID: 24990923 and Shrestha et al. Nat Neurosci 23(2); 281-292 (2020). PMID: 31959934
Data exclusions	None
Replication	Each experiment represents several independent cohorts, as described in the methods. All attempts at replication were successful.
Randomization	Mice were randomly allocated to experimental groups.
Blinding	Data was collected by researchers blind to genotypes. Data was analyzed by researchers blind to genotypes/ experimental manipulations.

Reporting for specific materials, systems and methods

We require information from authors about some types of materials, experimental systems and methods used in many studies. Here, indicate whether each material, system or method listed is relevant to your study. If you are not sure if a list item applies to your research, read the appropriate section before selecting a response.

Materials & experimental systems

n/a	Involved in the study
☐	☒ Antibodies
☒	☐ Eukaryotic cell lines
☒	☐ Palaeontology and archaeology
☐	☒ Animals and other organisms
☒	☐ Human research participants
☒	☐ Clinical data
☒	☐ Dual use research of concern

Methods

n/a	Involved in the study
☒	☐ ChIP-seq
☒	☐ Flow cytometry
☒	☐ MRI-based neuroimaging

Antibodies

Antibodies used

Rabbit anti-p S6 (S235/236) 1:1000 (Cell Signaling #4858)
Rabbit anti- p-S6K1 Thr389 1:500 (Cell Signaling #9205)
Rabbit anti- S6K1 1:500 (Cell Signaling #2708)
Rabbit anti-p eIF2α Ser51 1:300 (Cell Signaling #9721)
Rabbit anti- eIF2α 1:1000 (Cell Signaling #9722)
Mouse anti- β tubulin 1:5000 (Sigma #T8328)
Chicken anti-EGFP 1:500 (abcam #ab13970)
Rabbit anti-EGFP 1:300 (Thermo Fisher #G10362)
Rabbit anti-eIF4E 1:500 (Bethyl #A301-153A)
Rabbit anti-Mmp9 1:300 (abcam #ab38898)
Mouse NeuN 1:2000 (Millipore Sigma #MAB377)
Chicken anti-Somatostatin 1:300 (Synaptic Systems #366 006)
Rabbit anti- PKCδ 1:250 (abcam #ab182126)
Guinea pig anti-RFP 1:500 (Synaptic systems #390 004)
Mouse anti-puromycin 1:1000 (Millipore Sigma #MABE343)

Validation

Rabbit anti-p S6 (S235/236) 1:1000 (Cell Signaling #4858)
The p-S6 (S235/236) antibody (Cell Signaling #4858) is a monoclonal antibody produced by immunizing animals with a synthetic phosphopeptide corresponding to residues surrounding Ser235 and Ser236 of human ribosomal protein S6. This antibody is shown to work for immunohistochemistry (IHC) in human breast carcinoma cells in the vendor website. Primary literature citing use of this antibody for IHC in mouse brain tissue: Pristera, A., Blomeley, C. et al. PNAS 116(9): 3817-3826 (2019) PMID: 30808767

Rabbit anti- p-S6K1 Thr389 1:500 (Cell Signaling #9205)
The p-S6K1 (T389) antibody (Cell Signaling #9205) is generated by immunizing animals with a synthetic phosphopeptide corresponding to residues surrounding Thr389 of human p70 S6 kinase, and thus detects endogenous levels of p70 S6 kinase when only phosphorylated at threonine 389. Primary literature citing use of this antibody for western blot in mouse brain homogenate: Huynh, T., Santini, E., & Klann, E. J Neurosci 34(27): 9034-9039 (2014) PMID: 24990923

Rabbit anti- S6K1 1:500 (Cell Signaling #2708)
The t-S6K1 antibody (Cell Signaling #2708) is produced by immunizing animals with a synthetic peptide corresponding to residues surrounding the amino-terminus of human p70 S6 kinase. Primary literature citing use of this antibody for western blot in mouse brain homogenate: Huynh, H., Santini, E., & Klann, E. J Neurosci 34(27): 9034-9039 (2014). PMID: 24990923

Rabbit anti-p eIF2α Ser51 1:300 (Cell Signaling #9721)
The p-eIF2α (S51) antibody (Cell Signaling #9721) is generated using a synthetic phosphopeptide corresponding to residues surrounding Ser51 of eIF2alpha, and detects endogenous eIF2α only when phosphorylated at Ser51 and does not recognize eIF2alpha phosphorylated at other sites. Primary literature citing use of this antibody for western blot in mouse brain homogenate: Jiang et al. Nat Comm (2016). PMID: 27416896.

Rabbit anti- eIF2α 1:1000 (Cell Signaling #9722)
The t-eIF2α antibody (Cell Signaling #9722) is produced using a synthetic peptide against carboxy terminal sequence of eIF2α. This antibody is specific to total eIF2α protein. Primary literature citing use of this antibody for western blot in mouse brain homogenate: Jiang et al. Nat Comm 7:12185 (2016). PMID: 27416896

Mouse anti- β tubulin 1:5000 (Sigma #T8328)
The β-Tubulin antibody (Sigma #T8328) is a monoclonal antibody derived from the hybridoma AA2 produced by fusion of mouse myeloma cells and splenocytes from BALB/c mice immunized with purfied bovine tubulin. website states antibody reacts with beta-tubulin, types I, II, III and IV. Primary literature citing use of this antibody for western blot in mouse brain homogenate: Santini, E et al. Science Signal 10(504) (2017). PMID: 29114037

Chicken anti-GFP 1:500 (abcam #ab13970)
The GFP antibody from ABCAM (#ab13970) is a chicken polyclonal antibody raised against recombinant full length protein corresponding to GFP. Primary literature citing use of this antibody for IHC in mouse brain tissue: Shrestha et al. eLife 4: e08752; doi: 10.7554/eLife.08752. PMID: 26371510

Rabbit anti-GFP 1:300 (Thermo Fisher #G10362)
The GFP antibody from Thermo Fisher (#G10362) is a recombinant monoclonal antibody raised against full-length GFP protein. Primary literature citing use of this antibody for IHC in mouse brain tissue: Shrestha et al. Nat Neurosci 23(2); 281-292 (2020). PMID: 31959934

Rabbit anti-eIF4E 1:500 (Bethyl #A301-153A)
The eIF4E antibody (Bethyl #A301-153A) is generated by using an epitope specific to eIF4E that maps to a region between residue 1 and 50 of human eukaryotic initiation factor eIF4E. Primary literature citing use of this antibody for western blot in HEK293 cells: Cho, H. et al. Genes Dev 32(7): 555-567 (2018). PMID: 29654059

Rabbit anti-Mmp9 1:300 (abcam #ab38898)
The Mmp9 antibody (ABCAM #ab38898) is generated using full length protein corresponding to Mouse MMP9, and binds to Gelatinase-B, but does not cross react with other MMP family members (MMP-1, MMP-2, MMP-3). Primary literature citing use of this antibody for IHC in rat brain tissue: Qing-Feng, S et al. Arch Med Sci 15: 457-466 (2019). PMID: 30899299

Mouse NeuN 1:2000 (Millipore Sigma #MAB377)
The NeuN antibody (Millipore #MAB377) specifically recognizes the DNA-binding, neuron specific protein NeuN,, which is present in most CNS and PNS neuronal cell types of all vertebrates tested, and was generated using purified cell nuclei from mouse brain. Primary literature citing use of this antibody for IHC in mouse brain tissue: Ahrens, S. et al. Nat Neurosci 18: 104-11 (2015). PMID: 25501036

Chicken anti-Somatostatin 1:300 (Synaptic Systems #366 006)
The Somatostatin antibody (Synaptic Systems #366 006) is generated using synthetic peptide corresponding to AA 89 to 100 from mouse Somatostatin. The vendor website states that this antibody preferentially recognizes somatostatin-28, and only shows minor cross-reactivity to the unprocessed precursor protein and does not detect somatostatin-14. The antibody has been validated to use for immunohistochemistry, however no primary literature citing the use of this antibody has been listed by the vendor.

Rabbit anti- PKCδ 1:250 (abcam #ab182126)
The PKCδ antibody (abcam #ab182126) is a monoclonal antibody generated against recombinant fragment within mouse PKCδ aa500 to the C-terminus. Primary literature citing use of this antibody for IHC in mouse brain tissue: Fernandez, D.C. et al. Cell 175: 71-84 (2018). PMID: 30173913

Guinea pig anti-RFP 1:500 (Synaptic systems #390 004)
The RFP antibody (Synaptic Systems #390 004) is a guinea pig polyclonal antibody generated against the recombinant protein corresponding to AA 1 to 236 from mCherry (UniProt Id: X5DSL3). Primary literature citing use of this antibody for IHC in mouse brain tissue: Fink D. et al. Genesis 48(12); 723-9 (2010). PMID: 20853428

Mouse anti-puromycin 1:1000 (Millipore Sigma #MABE343)
The Puromycin antibody (Millipore Sigma #MABE343) detects puromycin incorporated into protein and was generated by immunizing animals with puromycin from Streptomyces alboniger. Primary literature citing use of this antibody for IHC in mouse brain tissue: Kim, S., & Martin, K.C. eLife 4(2015). PMID: 25569157

Animals and other organisms

Policy information about studies involving animals; ARRIVE guidelines recommended for reporting animal research

Laboratory animals	Mus musculus, iPKR knockin mice, Col1a1.TRE-GFP.shmir-eIF4E knockin mice, Floxed TRAP mice, Floxed tdTomato reporter mice, Som-Cre mice, PKCδ -Cre mice and C57Bl/6J mice from Jackson labs. Male and Female, 3-6 months old.
Wild animals	The study did not involve wild animals.
Field-collected samples	The study did not involve samples collected from the field.
Ethics oversight	New York University University Animal Welfare Committee and Institutional Biosafety Committee approved and provided guidance on the study protocol.

Note that full information on the approval of the study protocol must also be provided in the manuscript.